The Geochemistry and Runoff Process in Wolf Creek Research Basin, Whitehorse, Yukon Territory

Tianjiao Li

Thesis presented to the Faculty of Graduate and Postdoctoral Studies
in partial fulfillment of the requirements for the degree of
Master of Science in Earth Sciences

Department of Earth Sciences
Faculty of Science
University of Ottawa

Supervisor:
Dr. Ian D. Clark (Department of Earth Sciences)

Thesis Committee:
Dr. Danielle Fortin (Department of Earth Sciences)
Dr. Denis Lacelle (Department of Geography)
Dr. Tim Patterson (Carleton University)

© Tianjiao Li, Ottawa, Canada, 2013

Abstract

This study investigates the runoff process and groundwater behavior in a subarctic watershed called Wolf Creek Research Basin, in Whitehorse, Yukon Territory, Canada. This basin is underlain by discontinuous permafrost that is typical of high latitude watersheds. Goundwater supports the stream flow year round and dominated the hydrology in most of the study period as baseflow. The baseflow was concentrated in dissolved ions. However, the baseflow was diluted during the melt season in May and June of 2012. Multiple chemical and isotopic tracers were used to develop a robust three-component (groundwater, soilwater and precipitation) mixing model for runoff generation. The concentrations of weathering ions decreased with the increased discharge during the melt. Soilwater was responsible for about 60% of the streamwater on the hydrograph in the melt season. The infiltration of the meltwater from the snowpack and the thawed water from the seasonal frost to the baseflow existed. The tritium concentrations indicated that there was fast moving hydrogeological system within the basin. The baseflow was also characterized as relatively enriched in both ^{13}C and ^{14}C, and concentrated in DIC. DIC was the major loss of carbon in Wolf Creek Research Basin.

Résumé

Le pergélisol est grandement sous-jacent dans les bassins-versants à haute latitude. Cette étude examine le processus de ruissellement et le comportement des eaux souterraines dans un bassin-versant subarctique de Wolf Creek, à Whitehorse, territoire du Yukon au Canada. Les eaux souterraines soutenaient l'écoulement fluvial et dominaient l'hydrographe comme débit de base durant la majorité de la période d'étude. Le débit de base était concentré d'ions dissipés. Par contre, le débit de base était dilué durant la saison des fontes au mois de mai et juin 2012. Plusieurs traceurs chimiques et isotopiques étaient utilisé afin de développer un modèle de trois composants (eau souterraine, eau interstitielle de sol et précipitation) de ruissellement. Les concentrations de la désagrégation des ions diminuaient avec l'augmentation du débit durant la fonte. Les eaux interstitielles des sols étaient responsables de 60% de l'eau de ruisseau sur l'hydrographe durant la saison de fontes. L'infiltration de l'eau de fonte du manteau neigeux et l'eau du gel du débit de base existaient. Les concentrations de tritium indiquent qu'il y avait un système hydrogéologique qui se déplaçait à grande vitesse dans les limites du bassin. Le débit de base était aussi caractérisé comme étant enrichi en ^{13}C et ^{14}C, avec des concentrations en carbone inorganique dissous.

Acknowledgements

I would like to thank my supervisor Dr. Ian Clark for his endless support, guidance and funding for this project. I would also like to thank my colleague Matt Herod for his great help and guidance during fieldwork, lab work and data collection for my thesis. I am grateful for the help and diligent work for sample analysis from Paul Middlestead, Wendy Albi and Patricia Wickham in the G.G. Hatch Isotope Lab, and Ping Zhang and Nimal DeSilva in Geochemistry Lab. I would thank Gilles St-Jean and Normand St-Jean for their hard work in preparing the graphitization line. I should also thank Dr. Liam Kieser, Dr. Zhao Xiaolei and other supporting staff in the ISOTrace in the University of Toronton for their great effort in the AMS analysis. I would also thank Dr. Antoni Lewkowicz in the University of Ottawa and Dr. Philip Bonnaventure in Queen's University for offering shapefiles. I would give my thanks to Jeff Van Zandvoort and Emilie Herdes for their help in the fieldwork, and Richard Janowicz and Jonathan Kolot in the Water Resources Branch of Environment Yukon. I would also like to give my thanks Dr. Ratan Mohapatra, Sarah Agosta and other members in our research group, for their patience and support in past two years.

Finally, I would like to thank my family and my friends for their companion all these years. I would especially give my thanks to my parents for supporting and encouraging me to study aboard, and my boyfriend Kuan Jiang for his support and patience.

Table of Content

List of Figures

List of Tables

1 Introduction

Permafrost covers approximately 25% of the land area in the Northern Hemisphere. It is one of the key components of terrestrial ecosystems in cold regions (Yang *et al.*, 2010). The hydrology of arctic and subarctic northern watersheds is changing in response to the recent climate warming (Hinzman *et al.*, 2003; Serreze *et al.*, 2000). Phenomena like permafrost thawing and thermokarst (Lachenbruch and Marshall, 1986; Jorgeson *et al.*, 2006), reduction in area and number of closed–basin ponds (Riordan *et al.*, 2006), glacial recession (Kaseret *et al.*, 2006) and reduction in snow cover duration (Brown and Braaten, 1998) have been clearly observed (Walvoord and Striegl, 2007).

Unfortunately little attention has been paid to groundwater circulation in permafrost catchments, which may be an important link between climate variability and permafrost stability and (Yang *et al.*, 2010; Muskett and Romannovsky, 2009; Frey *et al.*, 2007; Utting, 2011). Permafrost degradation will result in a lower water table (Yang *et al.*, 2010), change in groundwater storage (Muskett and Romanovsky, 2009) and new pathways for contaminant migration (Dyke, 2011). Deeper circulation of water is also likely to increase the solute loading to creeks and rivers (Frey *et al.*, 2007; Utting, 2011).

Good conceptual models have been developed for permafrost-dominated watersheds (Petrone *et al.*, 2006; Boucher and Carey, 2010; Shanley *et al.*, 2002; Lyon *et al.* 2010; Carey and DeBeer, 2008; Obradovic and Sklash, 1986; Mcmara *et al.*, 1997; Laudon and Shymaker, 1997; Hoeg *et al.*, 2000; Rice and Hornberger, 1998). Stable isotope geochemistry, aqueous

geochemistry and hydrology have been widely used as tools for discovering the runoff processes and groundwater behavior. In this thesis a comprehensive picture of runoff processes and groundwater variations in the Wolf Creek watershed will be developed by using the advanced three-component hydrograph separations to interpret the seasonal variations of geochemical and isotopic tracers.

1.1 Permafrost

Permafrost is defined as ground (soil or rock) which remains at or below 0 ℃ for more than two consecutive years (NRC, 1988). The top of the permafrost is called the permafrost table. Talik is a layer or body of unfrozen ground in permafrost areas. The top layer of ground subject to annual thawing and freezing in areas underlain by permafrost is defined as the active layer (NRC, 1988). The thickness of the active layer depends on numerous factors such as air temperature, bedrock type, vegetation, slope, water content, etc., and may vary from year to year. Seasonal frost refers to the occurrence of ground temperatures below 0℃ for only part of the year.

The term continuous permafrost is applied to geographic regions where permafrost underlies more than 90% of the exposed land surface, with taliks found only in isolated locations such as beneath a deep lake or along the vent of a geothermal spring (Woo, 2012). Geographic regions where only some areas are underlain by permafrost while other areas are free of permafrost are described as having discontinuous permafrost. Sporadic permafrost refers to that permafrost occurred in isolated patches.

1.1.1 Hydrology in permafrost regions

Figure 1.1 illustrates a conceptual model for the hydrological cycle in permafrost regions. Precipitation occurs mainly in the form of snow in winter and rain in summer. In spring and summer, snow melts and the active layer thaws. Rainfall and snow meltwater saturate the surface layer. This surface water is stored for various lengths of time and may subsequently evaporate, infiltrate the ground or run off. Part of groundwater is stored underground as ice. Groundwater may discharge to various surface water bodies, or freeze in the ground along its flow path. Groundwater discharge, if it occurs in winter, freezes above ground or within the active layer. Otherwise, it emerges as springs or directly recharges streams, wetlands, lakes and seas (Woo, 2012).

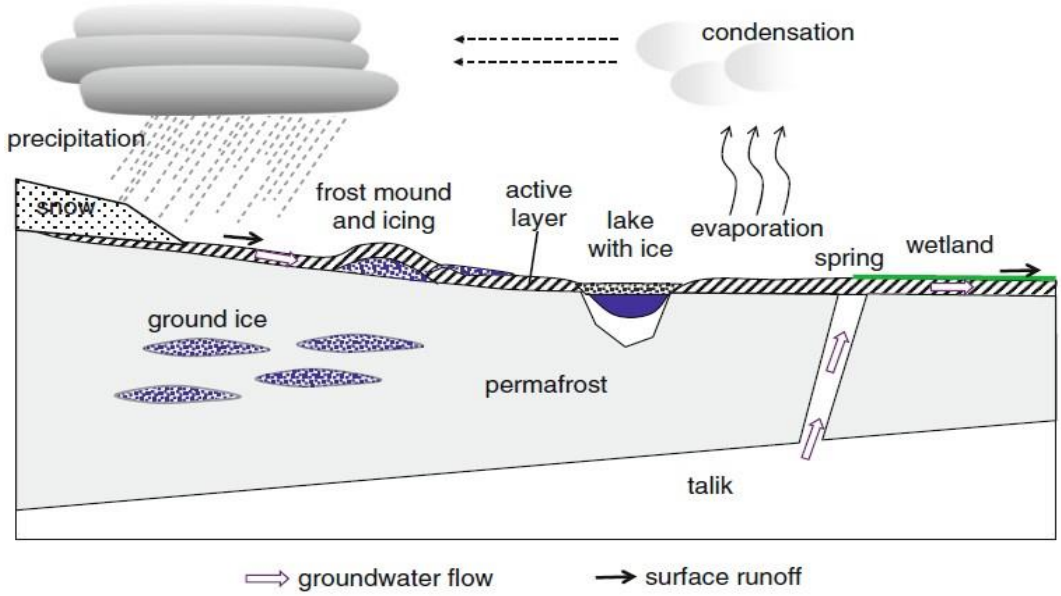

Figure 1.1 Conceptualization of the circulation and storage of water in permafrost regions, with emphasis on the effect of coldness (Woo, 2012)

Rouse (2000) claimed that tiny increases in the ground heating could create pronounced

changes in water storage and runoff pathways. The hydrology of the discontinuous permafrost terrain would be very particularly sensitive to the effects of the climate warming.

For permafrost-dominated watersheds, baseflows are low but stormflows can be quite high and rapid following snowmelt or rainfall. Permafrost acts as a confining bed in the subsurface that reduces soil water storage capacity and restricts flow paths (Hinzman *et al.*, 1991; Hinzman *et al.*, 1998; Kane *et al.*, 1991; Woo, 2000). The absence of permafrost allows deeper infiltration of precipitation and is thought to allow greater and more sustained baseflow and reduced stormflows (Slaughter and Kane, 1979; Woo, 1986; Woo and Winter, 1993).

Sub-arctic drainage basins are characterized by greater surface runoff and lower groundwater storage than temperate regions due to the presence of permafrost. Streamflow generation processes in permafrost regions are distinguished from more temperate regions in that: (1) snowmelt is typically the major hydrological event, although storms become more important in the late-summer and fall（Kane *et al.*, 2003; Spence *et al.*, 2011); (2) deep drainage is restricted by permafrost, and runoff is enhanced because of the near-surface water tables, and; (3) surface organic soils and preferential flow pathways allow a rapid means of supra-permafrost water to reach the stream (Carey *et al.*, 2013).

During the melt, most of the permafrost-underlain areas are saturated and water takes near-surface pathways to reach the stream. The pathways that runoff take are strongly controlled by the position of the water table as positive feedback occurs where faster runoff rates (and more runoff from precipitation events) occur when the water table is near the

surface (Carey and Woo, 2001; Quinton *et al.*, 2009). During a typical melt season in permafrost areas, precipitation and snowmelt dominate the hydrology of streamflow because the low storage capacity of the system produces high runoff rates.

1.1.2 Hydrogeology in permafrost regions

Permafrost reduces the permeability of the ground, thus acting as an aquitard or aquiclude. Groundwater is normally restricted to thawed zones (Woo, 2012). Active groundwater circulation can occur above, within and beneath the permafrost, known respectively as supra-permafrost, intra-permafrost and sub-permafrost groundwater (Figure 1.2; Tolstikhin and Tolstikhin, 1976; Williams and Waller, 1966; Woo, 2012). Seasonal frost in the active layer, icing and frost mounds are also associated with groundwater flow (Woo, 2012).

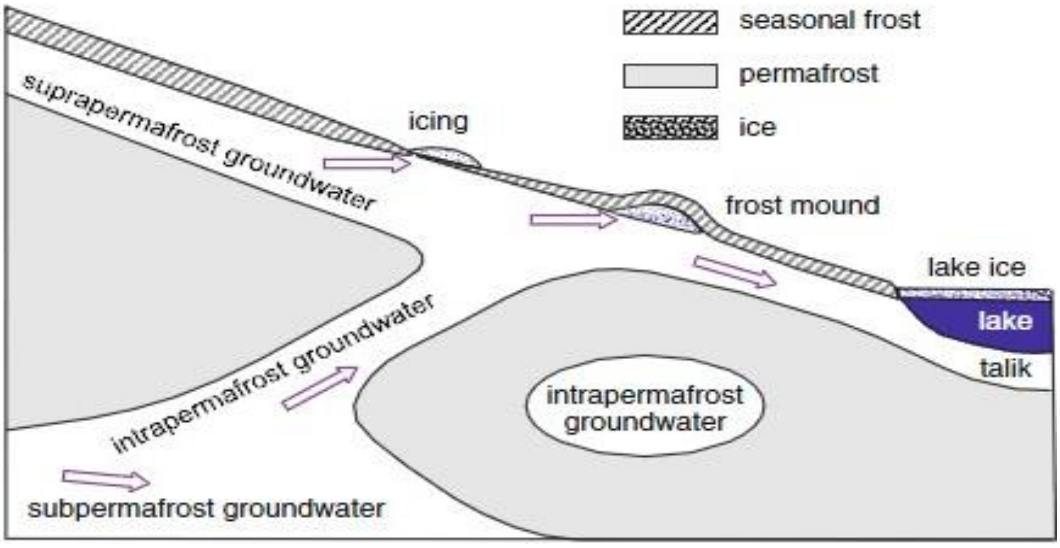

Figure 1.2 Occurrence of groundwater in permafrost: supra-permafrost (on top of the permafrost), intra-permafrost (within permafrost) and sub-permafrost (below permafrost) groundwater (Woo, 2012)

Supra-permafrost groundwater is found in the active layer, which forms in association with seasonal thaw events. It is mainly replenished by infiltration of meteoric water. High porosity materials and unconsolidated deposits at ground surface offer paths for water to recharge supra-permafrost groundwater. Intra-permafrost groundwater refers to taliks within the permafrost. Intra-permafrost groundwater is perennially unfrozen though the water can be <0℃ if it is high in concentrations of dissolved solids (Woo, 2012). The unfrozen zone can be an open talik, extending across the entire thickness of permafrost (van Everdingen, 1990), which connects intra-permafrost groundwater with the water above and below the permafrost. Sub-permafrost groundwater is the >0℃ water below the permafrost and typically has a long residence time in the aquifer that results in enrichment with dissolved ions. Sub-permafrost groundwater in discontinuous permafrost areas will connect to supra- and/ or intra- permafrost. Groundwater in permafrost zones discharges into rivers, tundra ponds and lakes, or onto the ground surface as springs and seeps.

Baseflow is the part of the streamflow supported by groundwater. In continuous permafrost areas, super-permafrost is the only source for baseflow, which means baseflow may terminate during a dry season or cold winter. In discontinuous permafrost regions, intra- and sub-permafrost groundwater can also support the baseflow, even if in a dry summer and freezing winter.

Leaching of soluble materials by surface and subsurface runoff can contribute to a difference in the chemical composition of the active layer and near-surface permafrost (Péwé and Sellmann, 1973; Leibman and Streletskaya, 1997; Kokelj, and Lewkowicz, 1999; Kokelj *et al.*, 2002; Kokelj and Burn, 2005). Entrapment of solutes by a rising permafrost table in conjunction with downward migration of ions along thermally induced suction gradients suggest that near-surface permafrost may be a sink for soluble materials (Kokelj and Burn, 2003). As a result, the geochemistry of the surface water, the soil and the groundwater may have changed significantly because of presence of permafrost and thawing of active layer.

Runoff processes and mechanisms are well understood in discontinuous permafrost regions in North America. Snowmelt dominates hydrochemical and hydrometric events in subarctic watersheds during spring melting. Prior to the melt, the baseflow is characterized by high dissolved ion concentrations associated with mineral weathering, reflecting deeper subsurface pathways, whereas nutrients and organic materials that indicate near-surface runoff are largely absent (Boucher and Carey, 2010). During the melt, permafrost and frozen ground restrict deeper drainage, enhancing near-surface water tables through widely present organic horizons (Slaughter and Kane, 1979; Carey and Woo, 2001; Carey and Quinton, 2004), enriching waters with nutrients, biologically active ions and dissolved organic carbon (DOC) (Carey, 2003).

Douglas *et al.* (2012) demonstrated that the thawing of permafrost leads to a decrease in the subsurface channelization of flows and changes in the timing and fluxes of organic matter and mineral weathering exports from northern watersheds. Permafrost-dominated catchments

have higher concentrations of dissolved organic carbon (DOC), but lower concentrations and fluxes of solutes compared to an adjacent watershed that is nearly permafrost free (MacLean *et al.*, 1999). Furthermore streamwater from catchments with the highest percentage of permafrost experienced the greatest increase of DOC during rain events. MacLean *et al.* (1999) interpreted this phenomenon to be the result of overland flow or subsurface flow through peat layers in valley bottoms of streams underlain by permafrost. Carey (2003) found that summer rainstorms could also increase stream DOC by increasing the proportion of hillslope drainage of the organic layer.

A study of the hydrogeochemistry of seasonal flow regimes in the Chena River, Alaska (Douglas et al, 2012) showed that rapid flushing of DOC, total dissolved nitrogen (TDN) and nitrate from surface soils occur during spring melt and summer rainstorms. These authors combined stable and radiogenic isotopic tracers to distinguish deep and shallow groundwater components. From winter to spring, the river water changed from low discharge derived from deep flows with a carbonate weathering signal to high discharge surface flow with a more silicate-dominated weathering signal . Spring flows had high organic matter content while organic matter was flushed in summer because of the increasing discharge from deeper flow paths.

1.2 Objectives and Thesis Structure

This thesis focuses on runoff processes in Wolf Creek Research Basin, identified based on streamflow hydrology and hydrogeology especially the groundwater behavior throughout the study period. Combining the hydrometric measurements with the geochemical and isotopic

data, comprehensive understanding of the runoff process and the groundwater behavior will be demonstrated in this thesis.

Objectives of this thesis are threefold:

(i) Identify geochemical tracers to monitor temporal variations in the streamflow and groundwater contribution to the discharge in a permafrost watershed, Wolf Creek Research Basin, Whitehorse, Yukon Territory.

(ii) Characterize end-member sources of the streamwater (groundwater, soilwater discharge and precipitation runoff) and calculate their distinct contribution to the streamwater.

(iii) Examine the seasonal variations of geochemical compositions, discharge and carbon export in the streamwater and groundwater component.

This thesis contains five chapters. Chapter One is the introduction and includes the site description of Wolf Creek Research Basin, Yukon Territory. Chapter Two introduces the background theory of lab analytical methods, geochemical and isotopic tracers, hydrograph separation and end-member mixing analysis. Chapter Three contains detailed results, which are discussed in Chapter Four. Chapter Five is the summary of the key findings and conclusions of the research.

1.3 Introduction to Wolf Creek Research Basin

The study area, called Wolf Creek Research Basin, is situated adjacent to the Alaska Highway approximately 15km from Whitehorse (60º30’N, 135º10’W), Yukon Territory, Canada (Figure 1.3). It is about 195 km^2 and at elevation form 800 to 2250 m. It is a typical subarctic

watershed that drains northeastern towards the Yukon River. The study of Wolf Creek Research Basin started in early 1990's. Initially the basin was studied for the impact of climate change. Now, it is an area for ecological and hydrological monitoring.

The climate of Wolf Creek Basin undergoes large temperature swings, and has a relatively low humidity and precipitation amount. Mean annual temperature in Wolf Creek Basin is -3℃. Arctic inversions are observed in the basin, which means an increase of temperature with height above surface. Mean annual precipitation is 300 mm to 400 mm per year, 40% of which is made up of snow. Several meteorological stations have been set up as this area.

Bedrock in the study area is mainly composed of sedimentary rocks, including limestone, sandstone and siltstone. Volcanic rocks also occur within the watershed, especially in the northern part. Bedrock outcrops over 50% to 60% of the area. The remaining 40% to 50% of the area is covered by glacial, glaciofluvial, alluvial, lacustrine, and windblown material into which present rivers have incised channels that are 70 metres deep or more (Seguin *et al.*, 1999).

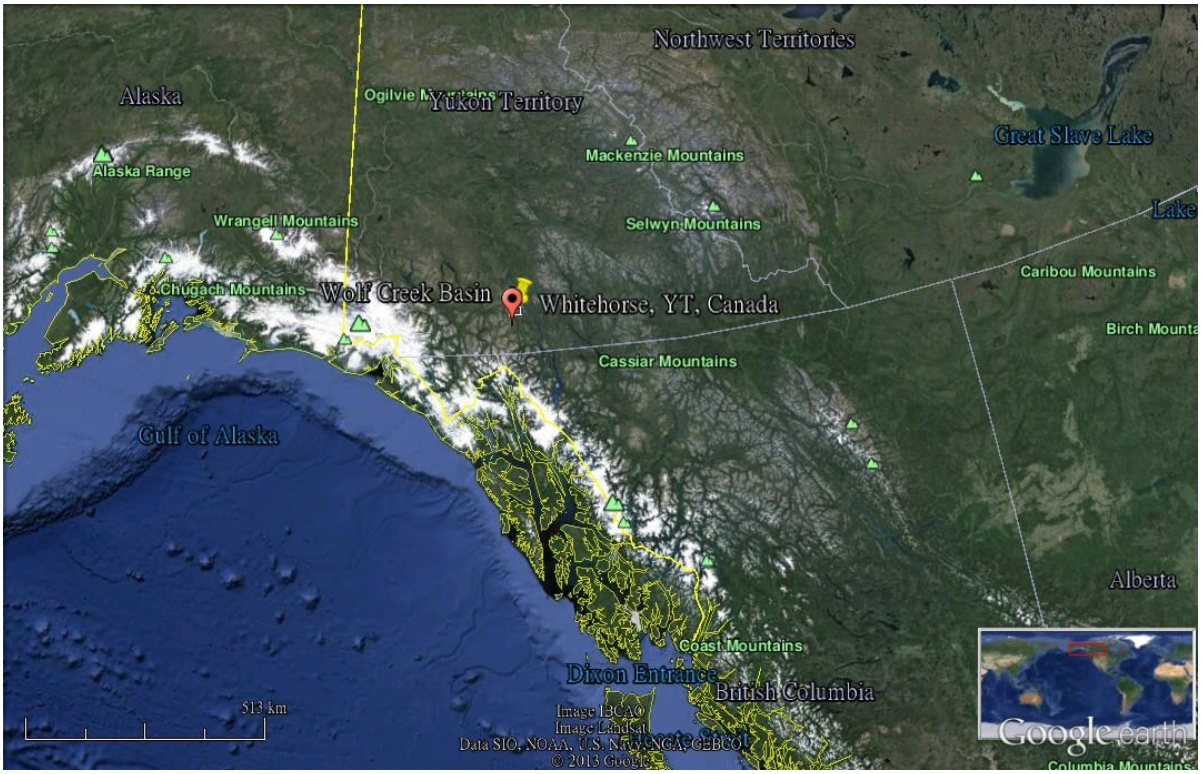

Figure 1.3 Locations of Wolf Creek Research Basin and Whitehorse, Yukon Territory, Canada (Google Earth version 6.2.2.6613)

The Wolf Creek watershed consists of three principle ecosystems: boreal forest (spruce, pine, aspen), subalpine taiga (shrub tundra) and alpine tundra with proportions of 22, 58 and 20 percent respectively (Francis, 1997).

Wolf Creek is a typical small, mountainous subarctic stream with minimum winter streamflows flows occurring during March or April. In addition to the groundwater contribution, significant lake storage within the basin contributes to minimum winter flows that are relatively high, in the order of 0.4 m^3/s (Janowicz, 1991). In contrast, the streamflow regime during spring snowmelt is characterized by peak flows of 10 to 20 m^3/s in late May or

early June. The basin is susceptible to intense summer rainstorm events that produce secondary peaks (Janowicz, 1986). Following extremely cold winters (defined as winters with at least 3 consecutive days with mean daily temperatures less than -40 ℃, as measured in Whitehorse), an aufeis formation developed at the outlet of Coal Lake can completely restrict outflow from the lake. The resulting ice dam has been observed to fail at the onset of snowmelt and, on occasion, may produce the annual peak flow in Wolf Creek (Jasek and Ford, 1997).

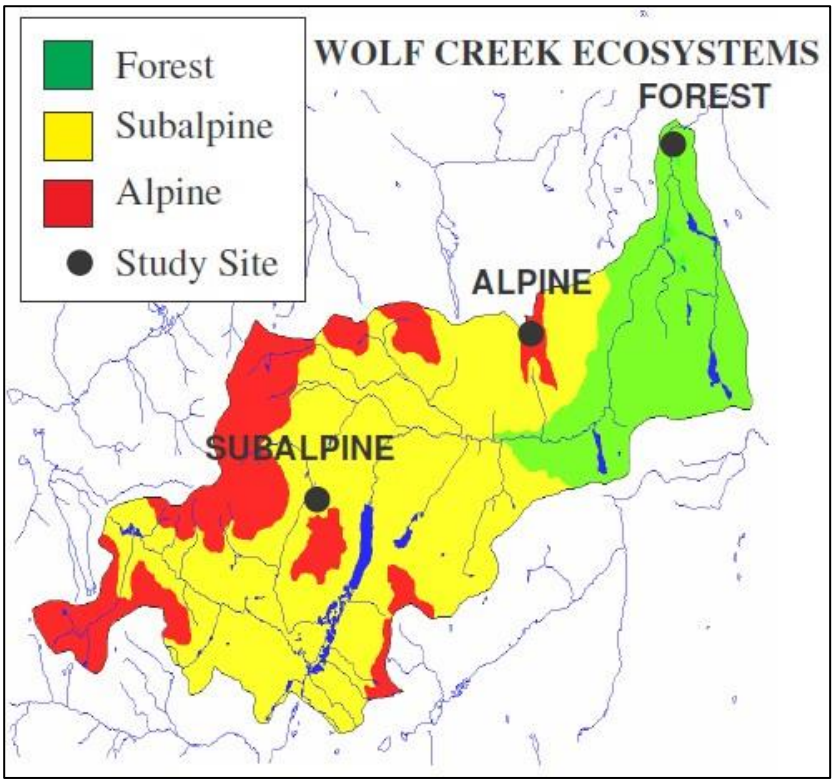

Figure 1.4 Ecosystems of Wolf Creek Research Basin (Pomeroy, 2004)

1.3.1 Permafrost in Wolf Creek Research Basin

Wolf Creek is located in a region of sporadic discontinuous permafrost (Figure 1.5). No detailed investigation into the local extent of permafrost has been undertaken. Seguin *et al.*

(1999) made a preliminary report suggested that permafrost underlay 25%-32% of Wolf Creek Basin. The basal temperature of snow (BTS) method was applied to map the permafrost in Wolf Creek Research Basin in 2002 and suggested that the best estimate of the area of the permafrost is 43% of the basin (Ednie, 2003). An areal description of the distribution of permafrost in the basin shows that above 1800 m a.s.l., all the terrain has a forecast permafrost probability >0.9 (i.e. continuous permafrost according to conventional mapping criteria (e.g. Heginbottom and Dubreuil, 1995), but that these areas make up only 5% of the entire basin (Figure 4). Most of the area between 1400 m and 1700 m is characterized by permafrost probabilities of 0.5–0.9 (widespread discontinuous permafrost), while between 800 m and 1400 m, the area is primarily sporadic discontinuous permafrost (0.1–0.5 probability). Below 800 m, the majority of the area is classified as isolated patches of permafrost (<0.1) (Lewkowicz and Ednie, 2004).

Permafrost has a profound impact on hydrology and chemistry of streams in subarctic areas such as Wolf Creek. Permafrost is present on the north-facing slopes, poorly drained areas, or where organic layers act as insulation. The presence of permafrost generally tends to increase with elevation; however, some other physical factors such as topography and vegetation will have an effect on the permafrost presence. Seguin (1998) suggested that discontinuous permafrost occurred from 1175 m on north-facing slopes and 1300 m on south-facing slopes. Continuous permafrost exists above 1500 m. Lewkowicz and Ednie (2004) pointed out that occurrences of thick (>10 cm thickness) organic mats are commonly found in parts of the basin underlain by widespread permafrost. The depth of the frost table was less than 2 m from the palsa stratigraphy (Coultish and Lewkowicz, 2003).

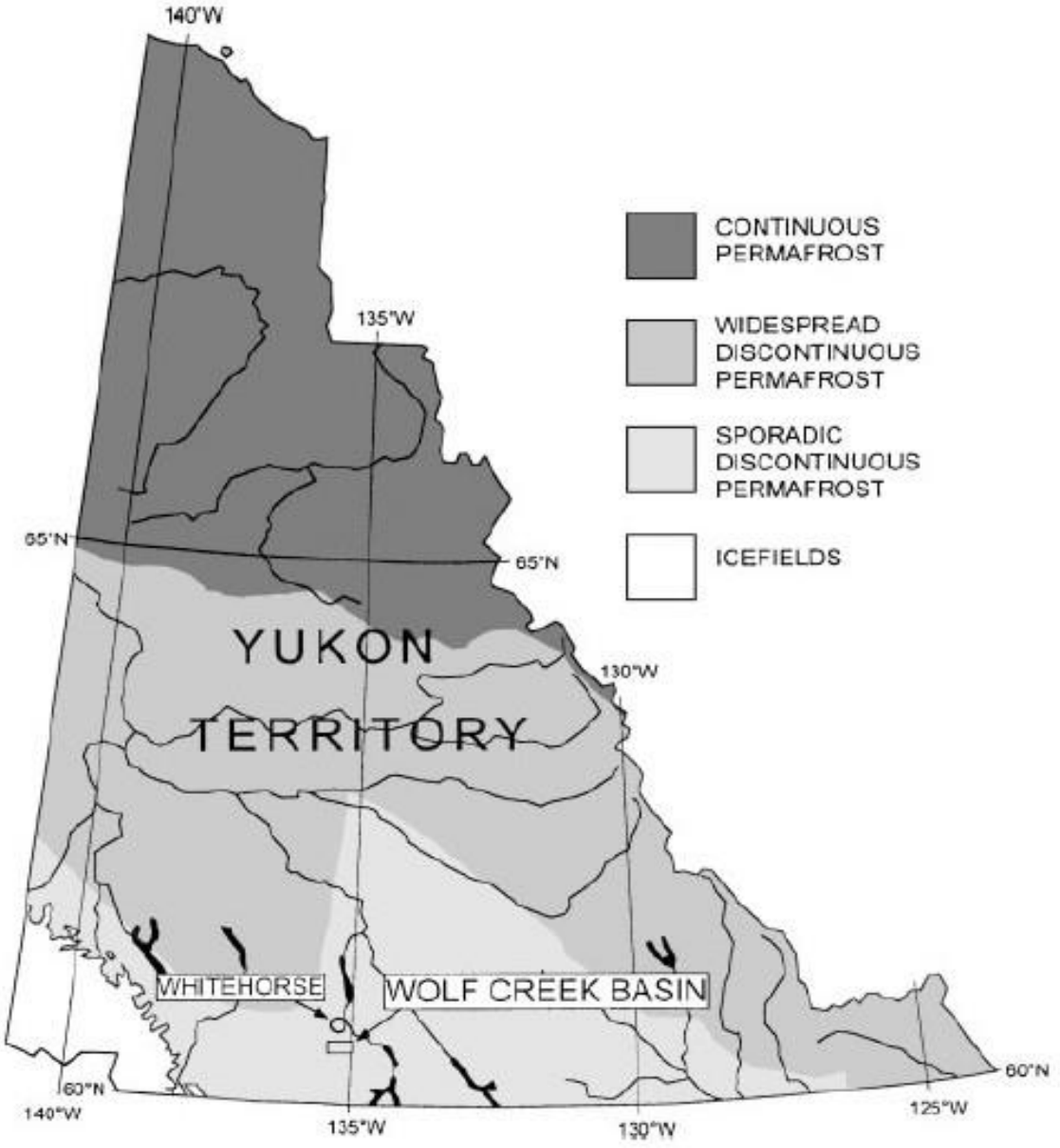

Figure 1.5 Location of Wolf Creek study basin relative to permafrost zones in the Yukon Territory, Canada (Lewkowicz and Ednie, 2004)

Several studies have focused on the Granger Basin (e.g. Carey *et al.*, 2013; Boucher and Carey, 2010), which is a sub-basin of Wolf Creek Research Basin (Figure 1.6). The Granger Basin is located in the northeastern part of Wolf Creek Research Basin and stands at a higher average

elevation than Wolf Creek average elevation. Permafrost is much more common in the Granger Basin, particularly in north-facing slopes and high-elevation areas. Lewkowicz and Ednie (2004) suggested that 70% -80% of the Granger Basin is underlain by the permafrost.

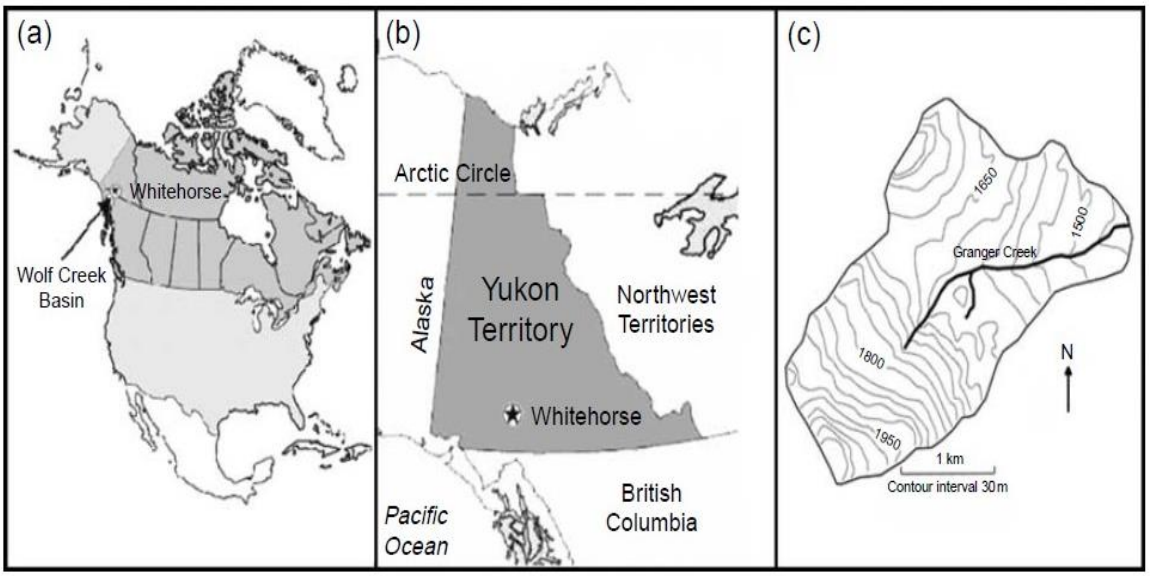

Figure 1.6 Location of Granger Basin (Boucher and Carey, 2010)

1.3.2 Hydrology in Wolf Creek Research Basin

Carey and Woo (2001) examined the water balance during the snowmelt and summer periods on four hillslopes in Wolf Creek Research Basin. Their results revealed strong variations in process magnitudes between sites that depend on factors such as frost, vegetation, soils and microclimate that controlled vertical and lateral fluxes. The snowmelt timing and rate were related to the radiation receipt, which was mainly controlled by vegetation, aspect and exposure on slopes. The snowmelt runoff was confined to hillslopes with organic soils underlain by an ice-rich base that prevented meltwater from percolating deeper into the ground. Porous organic material does not impede the water movement and lateral runoff

occurred once the storage capacity of the organic layer was exceeded. Evapotranspiration was the largest water loss. Differences in evapotranspiration were related to the length of the snow-free period, radiation receipt, vegetation and moisture in near-surface soils. The summer runoff included substantial flows from slopes where the water table was near the surface and was confined to wet organic-covered hillslopes.

In many northern, organic-covered terrains, the ground is saturated, or nearly saturated, with ice and a small amount of unfrozen water at the onset of snowmelt runoff in the spring and is fairly impermeable (Quinton and Gray, 2001). When the ground is thawing, the surface is close to the zero-degree isotherm. Horizontal hydraulic conductivity of saturated soil decreases exponentially with depth and the depth of the relatively impermeable frost table is critically important in controlling the rate of subsurface drainage from hillslopes (Quinton *et al.*, 2005). The unfrozen moisture storage shifts abruptly between 50-100 mm in depth from winter to summer, although soil temperatures remain close to the freezing point for rest of the year. The organic soil transmits water laterally during thawing. Following this period, the water movement is mainly vertical, between the ground surface and the underlying mineral sediment.

Boucher and Carey (2010) employed two loosely defined end-members, referred to as ‘new’ water and ‘old’ water, for hydrograph separation of Granger Basin streamwater. They concluded that old water is the dominant contributor during the freshet. Carey *et al.* (2013) confirmed this conclusion (Table 1.1) by using multiple year data for a two-component hydrograph separation and also confirmed that surface runoff is largely absent. Supra-permafrost groundwater, primarily flowing through near-surface organic soils, controls

the rate and timing of the snowmelt hydrology (Carey *et al.*, 2013). A possible explanation for the substantial groundwater contribution to the snowmelt hydrology is that infiltration meltwater displaces groundwater (Obradovic and Sklash, 1986). Organic soils in the basin can store the new water that displaces the old water. The authors hypothesized that during the early stages of the melt, there was limited transfer of water to the stream until the unsaturated storage capacity was satisfied and infiltrating meltwater supplied sensible heat to bring soils to 0 ℃ (although not necessarily fully thawed). At this time, lateral runoff pathways began to activate and mix with thawed old water. The contribution of old water gradually increased throughout the melt period (Carey and Quinton, 2004; Boucher and Carey, 2010) as mixing and displacement of old pre-event water occurred (Carey *et al.*, 2013).

Table 1.1 Volume weighted event and pre-event $\delta^{18}O$ concentrations for the study years (modified from Carey *et al.*, 2013)

Year	$\delta^{18}O_p$(‰)	$\delta^{18}O_{p-m}$(‰)
2002	-24.81±0.47	-24.5±0.18
2003	23.01±0.68	-20.7±0.22
2006	-24.26±0.71	-20.54±0.18
2008	-24.18±0.65	-21.19±0.16

1.3.3 Hydrogeochemistry in the Granger Basin

Boucher and Carey (2010) have demonstrated that ions in Granger Basin streamwater were diluted with the increased flow during spring melt events. Concentrations of cations like Ca^{2+} and Mg^{2+} were inversely correlated with discharge on a log-linear diagram (Figure 1.7). In contrast, biologically active K^+ and NO_3^- correlated poorly with discharge rates, and changes in their concentrations were more indicative of flow from near-surface organic horizons .

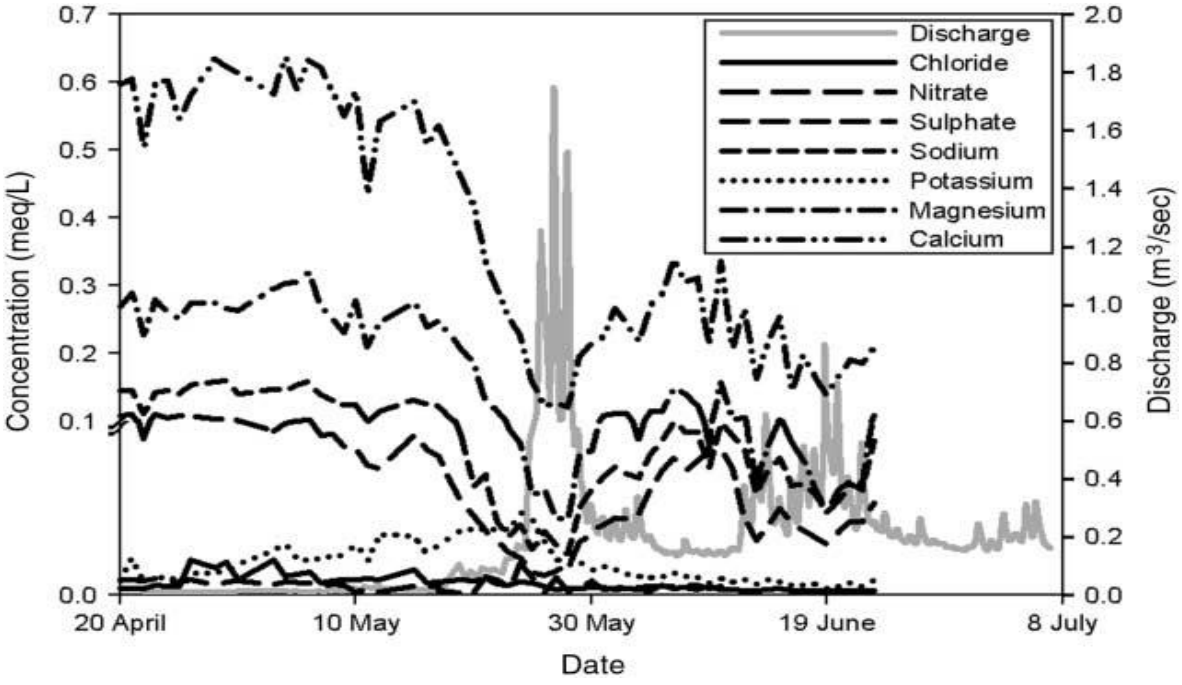

Figure 1.7 Time series of major ions and discharge (Boucher and Carey, 2010)

As aqueous potassium and calcium ions have different sources, the molar ratio of K^+: Ca^2 is often used to evaluate changes with depth in the soil profile of biologically active and inactive ions in solution (Boucher and Carey, 2010). In Granger Basin the molar ratio of K^+: Ca^{2+} increased with the near-surface flow before the peak freshet when the near-surface organic soil became saturated and generated the runoff. The pattern of K^+: Ca^{2+} was similar to that of DOC (Carey, 2003), which also peaked prior to the freshet and rapidly declined as labile carbon was flushed from soils (Boucher and Carey, 2010). The flushing of the DOC was likely a greater cause for the DOC decline than declining water tables, as evidenced by the 2003 patterns where DOC declined rapidly despite water tables being at or near the ground surface for a sustained period (Carey *et al.*, 2013).

While dissolved ions and DOC provide information about the flow pathways through which water travels to the stream, stable isotope data can tell the source of the water. Mixing diagrams of Cl^- *vs.* $\delta^{18}O$ and Cl^- *vs.* $\delta^{2}H$ have shown that streamflow before melt was primarily sourced from groundwater, with the meltwaters first recording an influx of soil water followed by snowmelt water. Towards the end of the study period, the stream values trended back towards the groundwater component, yet were no longer bound by the three proposed end-members (Boucher and Carey, 2010).

Carey *et al.* (2013) pointed out that the inter-annual variability in the patterns of the freshet discharge was considerable due to natural climate variability. Among all four monitored years, depleted patterns of $\delta^{18}O$ were found at the onset of freshet, indicating a mixing of pre-event (old) groundwater with snowmelt (event/new) water. Values typically decreased 1–1.5 ‰ $\delta^{18}O$, which was small compared with the snowmelt response of more temperate environments (Shanley *et al.*, 2002; Carey *et al.*, 2013).

2. Methodology

Numerous hydrogeological studies have involved geochemical and isotopic methods (e.g. Hoeg *et al*., 2000; Rice and Hornberger, 1998; Boucher and Carey, 2010). In this study, traditional physical measurements of streamflow and conventional geochemical and isotopic methods were combined with some novel geochemical and isotopic methods. Tritium (T) and radiocarbon (^{14}C) data were provided together with the geochemical results, dissolved inorganic carbon (DIC), $\delta^{18}O$, $\delta^{2}H$, $\delta^{13}C$ in DIC and the discharge data. This approach has produced a more robust analysis of runoff processes and groundwater behavior in Wolf Creek Research basin during the spring melt. These methods are presented in this chapter along with their theoretical basis.

2.1 Sampling Methods

Fieldwork was conducted from April to October in 2012. Water samples were collected through that period in order to identify end-members within the watershed. Three types of water were collected for Wolf Creek Research Basin. A variety of water sources were sampled within the watershed, including surface drainage, lakes, quarry ponds, snow, wells, springs and active layer discharge (Figure 2.1). In addition, weekly water samples from Wolf Creek mainstream were taken where the creek was accessible from the Alaska Highway. Finally, precipitation samples were collected in Whitehorse from June to October.

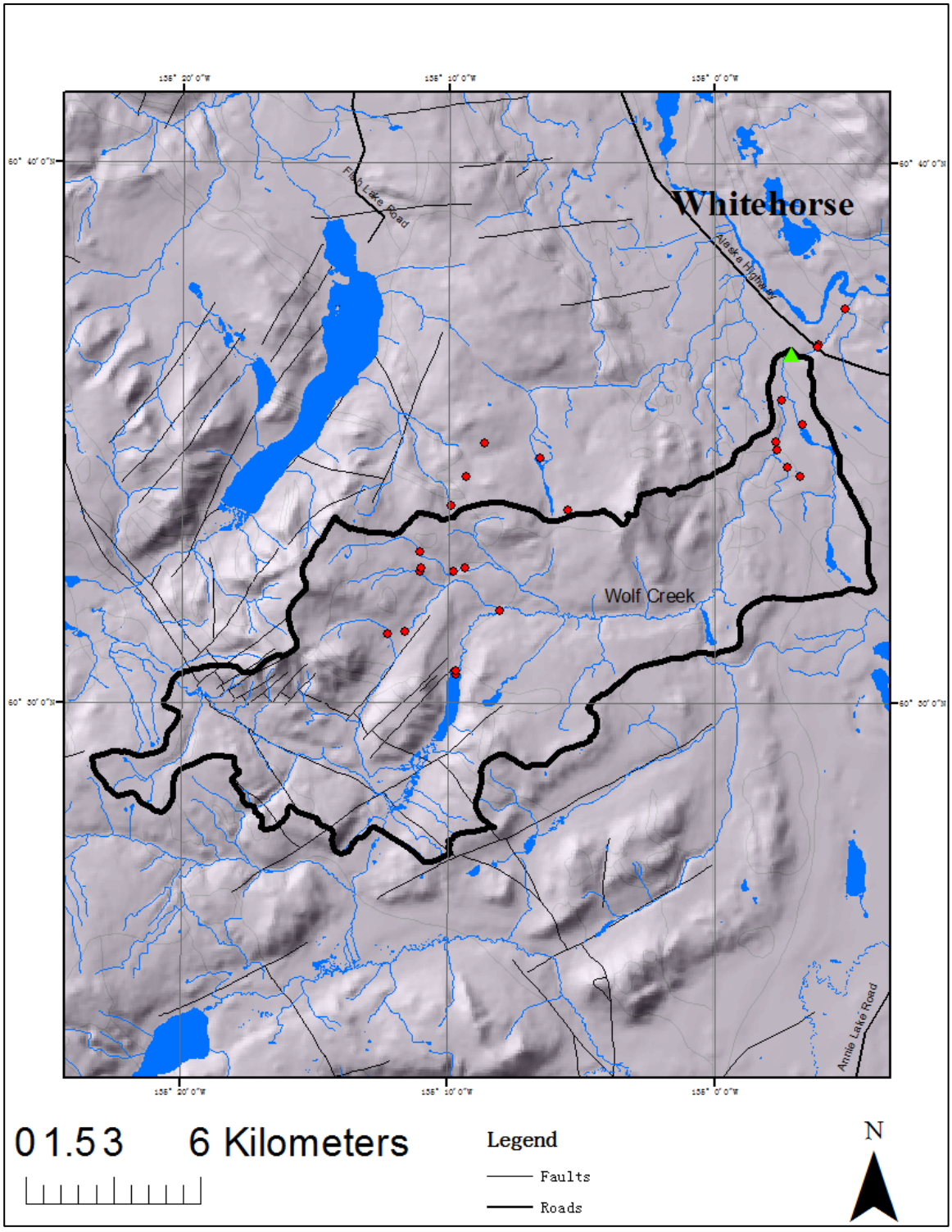

Figure 2.1 Summer sampling sites in Wolf Creek Research Basin

Alkalinity, pH, conductivity, temperature and oxidation-reduction potential (ORP) were

measured in the field using YSI Professional Plus Handle Multi-parameter Instrument. Water was filtered with 0.45μm filters and collected in 60ml centrifuge tubes and 40 ml I-Chem EPA vials for geochemical and isotopic analysis. Extra water samples were stored in HDPE bottles.

2.2 Geochemical Analytical Methods

Samples were shipped to the University of Ottawa for analysis. All samples were analyzed for major ion concentrations, $\delta^{18}O$ and $\delta^{2}H$, dissolved inorganic carbon concentrations (DIC), $\delta^{13}C$ in DIC, dissolved organic carbon (DOC) and $\delta^{13}C$ in DOC. Some of them were also analyzed for $\delta^{14}C$ in DIC and tritium concentrations.

Major ion concentrations were analyzed in the Geochemistry Lab at the University of Ottawa. Water samples were measured by Inductively Coupled Plasma Emission Spectroscopy (ICP-ES), while anion concentrations were measured with a Dionex-100 ion chromatograph (IC) in Ottawa. Filtered water samples were acidified in the lab before applying on the ICP-ES.

$\delta^{18}O$ and $\delta^{2}H$ were analyzed by Laser Absorption Spectroscopy (LAS) using a Los Gatos Research (LGR) Isotopic Water Analyser Model 912-0026. Routine precision for hydrogen is ±1‰and for oxygen is ±0.25‰. Results were normalized to Vienna Standard Mean Ocean Water (VSMOW).

DIC and DOC were measured using an OI Analytical Aurora Model 1030W TIC-TOC Analyzer interfaced to a Finnigan Mat DeltaPlusXP Isotope Ratio Mass Spectrometer (St-Jean,

2003) for analysis by continuous flow. Data were normalized using three different internal organic standards. Results were normalized to Vienna Pee-Dee Belemnite (VPDB) standard. The analytical precision is 2% of the DIC/DOC elemental concentration (in ppm), and ± 0.2 per mil for $\delta^{13}C$ isotopic composition. Isotope results were respect to Vienna Pee-Dee Belemnite (VPDB) standard.

CO_2 gas was extracted from DIC and then graphitized as a preparation process for the ^{14}C analysis on the Accelerated Mass Spectrometry (AMS). The graphitization line is newly set up in the Department of Earth Sciences of the University of Ottawa. Alfa Aesar iron powder (-200 mesh) was added as catalyst to reduce conversion time from CO_2 to graphite. The graphitization was conducted in a H_2 environment. The standard was NIST-SRM 4490C oxalic acid powder and also graphitized on the graphitization line. The $^{14}C/^{12}C$ ratios were measured by Accelerated Mass Spectrometry (AMS) at the Isotope and Rare Atom Counting Equipment (ISOTrace) Laboratory in University of Toronto. The $\Delta^{14}C$ values were corrected by the $\delta^{13}C$ values analyzed by TIC-TOC and reported as final results. Unfortunately, the streamwater sample on May 17th was lost during graphitization.

Tritium activity was analyzed by the electrolytic enrichment method in Isotope Tracer Technologies Inc. in Waterloo, Ontario. 150 ml of water samples were deionized by adding mixed bed ion exchange resin and then placed into metal cells for electrolytic enrichment. Enrichment proceeded for about one week until volumes of samples were around 15ml. One gram of sodium peroxide (Na_2O_2) was poured into the water samples before the electrolytic enrichment and got rid of water by final distillation. The distilled and enriched water samples counted on the Liquid Scintillation Counters (LSC) by adding the Ultima Gold LLT^{TM} (low

level tritium) cocktail. Counting results were reported in Tritium Units (TU) for tritium concentrations. 1 TU = 3.221 Picocurries/L = 0.11919 Becquerels/L = 1 ^{3}H per 10^{8} hydrogen atoms (IAEA, 2000).

2.3 Hydrograph Separation

The relationships among recharge, storage and discharge of a watershed can be discovered from compositional variations in the streamflow during rainy and/or dry seasons. In basin budget studies, it is important to assess the proportion of precipitation that actually recharges the groundwater, i.e. the percentage of precipitation that actually recharges groundwater and that which is lost by surface runoff. The rate at which the baseflow runoff changes over time is a measure of the actively circulating groundwater in the basin. Stream hydrograph separation into baseflow and storm runoff components is the basic tool in determining the components of discharge from a catchment (Clark and Fritz, 1997).

The principle of isotopic hydrograph separation is based on the contrasting isotopic compositions of different sources of water. The groundwater in the basin will have an isotopic composition that reflects the long-term averaged input value whereas storm water will have a discrete δ-value falling somewhere within the range of the mean annual value (Clark and Fritz, 1997). Isotopes, tracing elements, total dissolved solids (TDS) or electrical conductivity (EC) can be used in the hydrograph separation as they will all vary within the baseflow or the stormflow.

Two- and three-component hydrograph separations are commonly applied in small-scale

catchment studies, particularly during rainfall or storm events, to identify the origin, timing, and pathways of surface and subsurface runoff, with the primary objective being the evaluation of streamflow generation mechanisms (Cooper *et al.*, 1993). Two-component method are based on an assumption that only two major components participate in the runoff: groundwater baseflow and rainfall; old water and new water, or; pre-event water and event water.

The equation for the flux of two-component hydrograph separation is:

$$Q_t=Q_{gw}+Q_r$$

Based on isotopic mass balance, the equation becomes:

$$Q_t*\delta_t=Q_{gw}*\delta_{gw}+Q_r*\delta_r$$

where Q is the discharge component, and the subscripts represent total stream flow (t), pre-storm groundwater (gw) and storm runoff (r). δ is the isotope concentration. The three-component approach takes the soil water into account. Two parameters are used in three equations to resolve the three component of total discharge, like $\delta^{18}O$ and Si. The equations are:

$$Q_t=Q_r+Q_s+Q_{gw}$$

$$Q_t*\delta_t=Q_{gw}*\delta_{gw}+Q_r*\delta_r+Q_s*\delta_s$$

$$Q_t*C_t=Q_{gw}*C_{gw}+Q_r*C_r+Q_s*C_s$$

where the subscript s is the soilwater component and C is the concentration of geochemical tracer.

Many studies have used isotopic hydrograph separation characterize hydrological process within a catchment. Although the value of incorporating groundwater or soil water isotopic

information in the separation analysis has been known for some time (Dewalle *et al.*, 1988; Ogunkoya and Jenkins, 1993; Hinton *et al.*, 1994; McGlynn *et al.*, 1999) only a few studies have actually used this approach, mainly because data collection is time consuming and difficult, especially during winter conditions with deep snowpacks and extensive soil frost (Laudon *et al.*, 2004). Laudon *et al.* (2004) found that water samples from suction lysimeter 70 cm below the surface were similar to water from the pre-melt water in $\delta^{18}O$ values. This similarity indicated that soil below 70 cm at depth was not affected by snowmelt water and lateral transport of event water happened mainly above 70 cm in soil.

A simple two-component mixing model is used in hydrograph separation to figure out the contribution from old and new water, where old water is the water that has been stored in the watershed (i.e. soil moisture and groundwater) and new water is event driven precipitation or snowmelt. Advanced three-component hydrograph separation techniques separate the old water into soil water and deep groundwater. The two-component mixing model can be accepted when no sample is from deep groundwater. Due to the heterogeneity of soil water, it is difficult to get an accurate and precise chemical signature of old water. Typically, the composition of stream water during low flow periods between storms is assumed to represent an integrated sample of the old water in the basin. The signature of precipitation for the event is used as the new water end-member (McKenna, 1989).

2.4 Isotopic Tracing

Isotopic tracers are often applied with geochemical tracers like major ions, trace elements, DIC, etc. They can label interactions within specific material and environment. Isotope

hydrograph separation applied in conjunction with physical monitoring, has been helpful for establishing or redefining conceptual models of water delivery on the hillslope or small catchment scale (Gibson *et al.*, 2005). Michel and Fritz (1978) claimed that very large isotope variations are preserved in permafrost waters and are considered to be the result of changes in climate and/or fractionation during freezing process.

2.4.1 Oxygen and hydrogen stable isotopes

Oxygen and hydrogen isotopic tracers have been applied widely in the field of hydrology in recent decades. ^{18}O and ^{2}H can behave conservatively, which is the threshold for this technique. Isotope fractionation produces a natural labeling effect within the global water cycle that has been applied to the study of a wide range of hydrological and climatic processes at the local, regional, and global scales (Gibson *et al.*, 2005). This technique takes advantage of significant differences in the stable isotope concentrations between different events, seasons, sources and etc. In the streamflow generation study, the proportional contributions of old and new water to streamflow can be evaluated (Cooper *et al.*, 1993).

Isotopically depleted waters are found in cold regions while enriched waters are characteristic of warm areas. This is a basic rule for distinguishing recharge sources for water bodies. $\delta^{18}O$ and $\delta^{2}H$ values for groundwaters, precipitation, lakes and rivers, etc, can be rather different because of different origins and transport process. Snowmelt or cool rains in spring is one of the reasons that make the isotopic biases between groundwater and precipitation.

$\delta^{18}O$ was used to trace the hydrological process of streamflow in the Imnavait Creek, Alaska

(Cooper *et al.*, 1993). A shift in $\delta^{18}O$ was observed in the stream water from -30.3‰ on the first day of streamflow to -22.5‰ at the end of the snowmelt. This result suggested a mixing between snow and soil moisture, however, was impossible based on other isotope data. Isotropic fractionation took place during the phase change from solid to liquid dominates the isotopic variation in streamflow during the snowmelt. This phenomenon implicated a wave like mechanism for forcing old water into the stream channel (Cooper *et al.*, 1993). Evaporation was the main factor in the hydrological cycle and pointed out that isotopic fractionation might lead to the overestimate of mixing between snowmelt and soil water.

2.4.2 Tritium

Tritium is a radioactive hydrogen isotope that occurs naturally and and is a byproduct of nuclear power plants operations. Atmospheric tritium is generated during by cosmic ray bombardment according to following reaction:

$$^{14}N + n \rightarrow {}^{12}C + {}^{3}H,$$

where n is the neutron from cosmic radiation. The natural tritium concentration in atmosphere is uncertain as few measurements were conducted before the nuclear testing.

A neutron flux is present in the subsurface from spontaneous fission of U, which can result in ^{3}H production through the fission of ^{6}Li according to:

$$^{6}Li + n \rightarrow {}^{3}H + \alpha.$$

Considering the short half-life of tritium there is likely insufficient time for significant accumulation by this process.

Tritium decays to ^{3}He by release of a beta particle according to the bata release of tritium

decay:

$$^{3}H \rightarrow {}^{3}He + \beta^{-} .$$

The ^{3}H-^{3}He dating method is applied in dating modern waters within 50 years.

There was thermonuclear bomb testing from 1950 to 1980 in several countries. The final year of megaton tests was 1962 and generated a huge peak in tritium, which appeared in precipitation in the spring of 1963. The 1963 peak became a tracer in many hydrological studies (Figure 2.2). Tritium has a half-life of 12.3 years, so the tritium level in precipitation is now approaching the natural cosmogenic value.

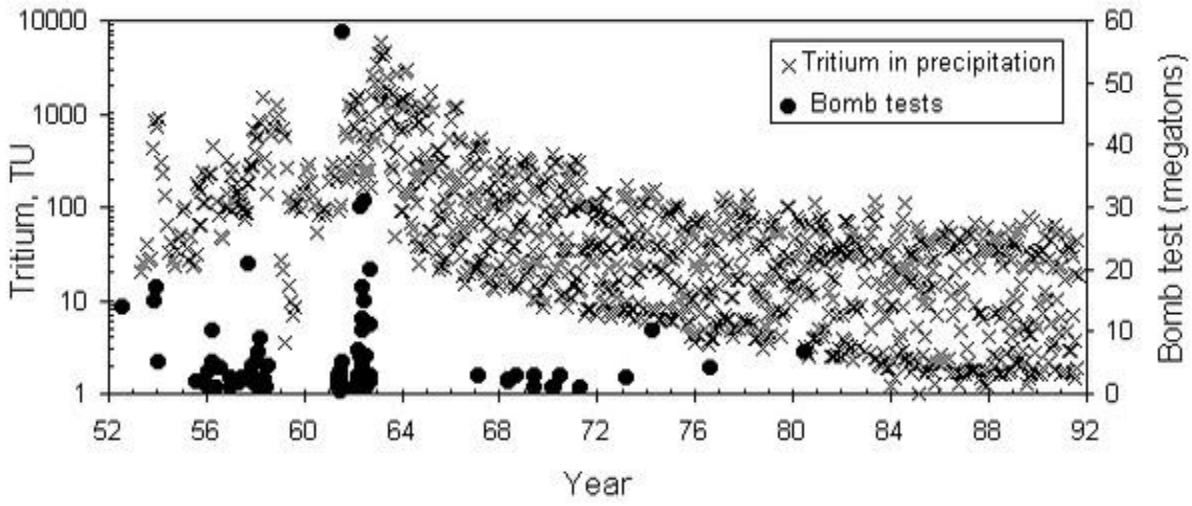

Figure 2.2 Tritium in precipitation from thermonuclear bomb tests since 1952. Tritium data for selected stations in North America and Europe, from the IAEA GNIP database (Clark and Fritz, 1997).

2.4.3 Carbon isotopes

The stable carbon isotope ^{13}C is an excellent tracer of carbonate evolution in groundwater

because of the large variations in the various carbon reservoirs (Clark and Fritz, 1997). Atmospheric CO_2 with $\delta^{13}C$ of 7‰ VPDB is stabilized in soil by organics and dissolved in infiltrated water. The $\delta^{13}C$ of soil CO_2 in most landscapes dominated by C_3 plants is generally about -23‰ compared to -9‰ values of $\delta^{13}C$ in landsapes covered by C_4 vegetation (Clark and Fritz, 1997). In the Yukon, soil CO_2 is assumed to be derived primarily from C_3 vegetation (Utting, 2011).

DIC and $\delta^{13}C_{DIC}$ in groundwater are related to the weathering in the soil or aquifer. Marine carbonates have $\delta^{13}C$ values close to 0 according to VPDB as the ^{13}C contents are similar to the VPDB reference. The more carbonate is dissolved in groundwater, the more enrichment of $\delta^{13}C_{DIC}$ occurs. How much carbonate is dissolved depends on the openness of the system Open conditions have a continual soil CO_2 supply and the $\delta^{13}C_{DIC}$ value is generally between 15‰ and 18‰ under open condition, while $\delta^{13}C_{DIC}$ is close to 12‰ in closed conditions. Greater enrichments can be generated through continuous exchange between DIC and the carbonate matrix, and through incongruent dissolution of dolomite (Utting, 2011). Open and closed system dissolution of carbonate can be distinguished by differences in P_{CO2} and DIC concentrations in groundwater (Clark and Fritz, 1997). High P_{CO2} and DIC characterize open system dissolution in contrast to low values in closed system dissolution. As $\delta^{13}C$ increases during both open and closed system evolution, this parameter may not be diagnostic. However ^{14}C measurements can be useful in evaluation the degree of openness.

Radiocarbon can be produced in the upper atmosphere via the following nuclear reaction:

$$^{14}N + n \rightarrow {}^{14}C + p$$

where n means neutron and p means proton. Then ^{14}C oxidizes to carbon dioxide and enters

the water, soil and organic matter. The largest storehouse of ^{14}C is by far the oceans, in the form of bicarbonate (HCO_3^-) (Table 2.1). Accumulation in the troposphere and the hydrosphere/biosphere is balanced by radioactive decay and burial (Clark and Fritz, 1997).

Table 2.1 Terrestrial carbon reservoirs (Berner and Lasaga, 1989; Clark and Fritz, 1989)

Form	Mass (10^{18}g)	Living biomass equivalent
^{14}C-free		
Marine Carbonates	60,000	107,000
Sedimentary Hydrocarbon	15,000	26,800
Recoverable Coal, Oil and Gas	4	7.1
^{14}C-active		
Oceanic DIC	42	75
Dead Vegetation	3	5.4
Atmospheric CO_2	0.72	1.3
Life on Earth	0.56	1

Neutron fluxes in the subsurface from spontaneous fission of uranium and other elements can produce hypogenic ^{14}C by neutron activation of ^{14}N or neutron capture by ^{14}O and α decay (Clark and Fritz, 1997). However, the subsurface neutron flux is very low. Hypogenic radiocarbon production is negligible as a radiocarbon reservoir.

Anthropogenic activity has a large impact on the atmosphere ^{14}C concentration. The consumption of fossil fuel, which contains almost no ^{14}C, releases dead carbon into the atmosphere while diluting ^{14}C. Conversely, atmospheric weapons testing and nuclear power

plant have been releasing radiocarbon since 1950s and increasing the radiocarbon activity considerably. Especially a doubling peak was observed in 1963.

^{14}C has a half-life of 5730 years and been widely used as a tracer for calculating the groundwater travel time since recharge. The range for dating with ^{14}C is <100 years to 30000 years. The radiocarbon dating theory is based on the measurement of radiocarbon loss in a given sample. There are two key assumptions for the system: (1) the initial concentration of the parent is known and has remained constant in the past; (2) the system is closed to subsequent gains or losses of the parent. (Clark and Fritz, 1997)

If the groundwater had no gains or losses of ^{14}C along its flowpath, which means that the ^{14}C activity remains as same as the ^{14}C activity in the soil, then the decay of ^{14}C can be used as a measure of groundwater age. The major difficulty with using ^{14}C for age dating in dissolved inorganic carbonate (DIC) is accounting for the addition of dead carbon which can greatly dilute the ^{14}C concentration and hence increase the apparent ^{14}C ages (McIntosh *et al.*, 2012; Geyh, 2000*;* Zhu and Murphy, 2000*)*. The reactions that may dilute radiocarbon in DIC with dead carbon include carbon mineral (calcite, dolomite) dissolution in recharge areas and oxidation of old organic matter along flow paths or within the aquifer etc.

3. Results

The results are presented in five sections. The first section presents the temperature records.

The second section documents the precipitation records. The third section presents the geochemistry and isotope results from the summer water sampling. The forth section includes the discharge records, geochemistry and isotope results of the streamwater from Wolf Creek. The last section provides the results of hydrograph separation analysis.

3.1 Temperature

Temperature records for the spring and summer of 2012 were collected for Whitehorse by Environment Canada (Figure 3.1). As the spring arrived in April, the temperature started to increase gradually. Although the maximum temperatures reached 10 ℃ in April and May, the minima were still below zero. During the summer (June to August), the temperatures were higher as the mean temperatures were around 15 ℃. The minimum temperatures were all above 0 ℃ and sometimes the maxima were nearly 30 ℃. Temperatures declined gradually from the end of August along with the coming of fall. The temperatures dropped quickly in September and October. The mean temperatures in Whitehorse remained below 0℃ from mid-October.

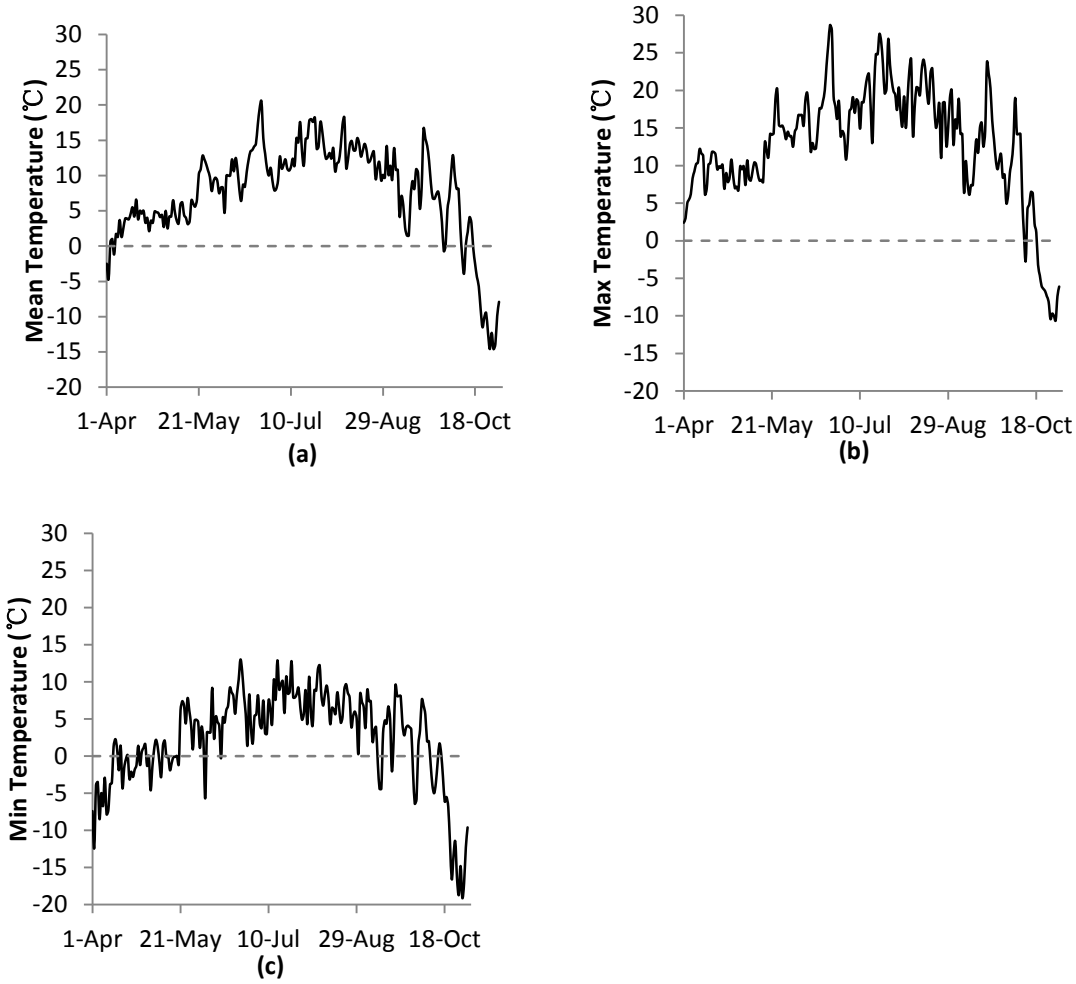

Figure 3.1 Temperature records for Whitehorse from April to October in 2012，(a) Mean Temperature (b) Maximum Temperature (c) Minimum Temperature

3.2 Precipitation

Precipitation data for Whitehorse during the study period was taken from the website of Environment Canada (Figure 3.2). `There were more frequent precipitation events in the summer period (July-September) than in the spring (April –June). Snowstorms did not return until October. The heaviest rainstorms occurred at the end of June and beginning of July, and accumulated over 10mm per day.

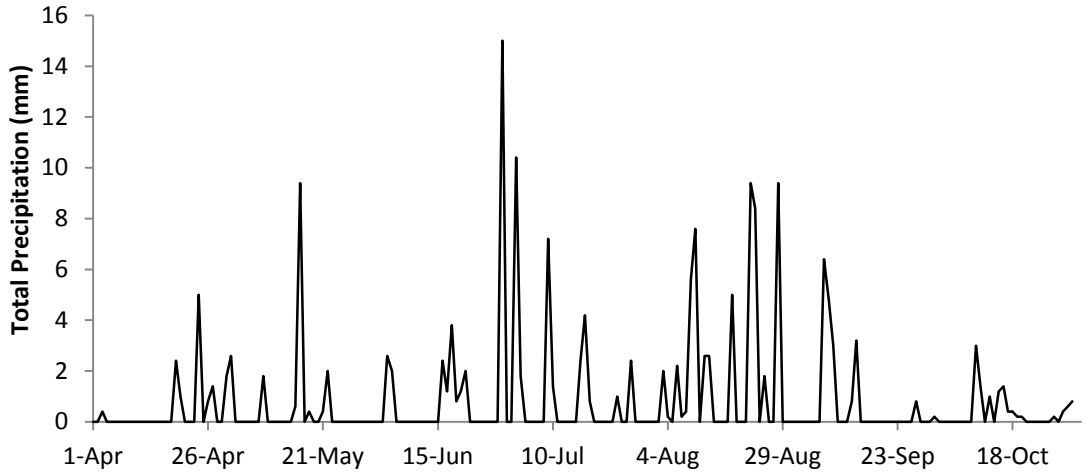

Figure 3.2 Precipitations in Whitehorse from April to October in 2012

Precipitation samples were collected in the field from June to September. Dissolved ion concentrations were less than 1 ppm (Figure 3.3). The values of ^{18}O and δ^2 H were close to the local meteoric water line (LMWL) determined by Lacelle (2011) as shown in Figure 3.4. The local meteoric water line (LMWL) generated from precipitation in Whitehorse and Mayo has a slope around 6. Surface water from lakes in the Yukon defines a local evaporation line (LEL) with a slope around 4. The intersection point of the LEL and LMWL defines the average isotope composition of unmodified mean annual precipitation (Anderson, 2005). Evaporation in Wolf Creek catchment was assumed to be low due to the cool and humid conditions and vegetation coverage.

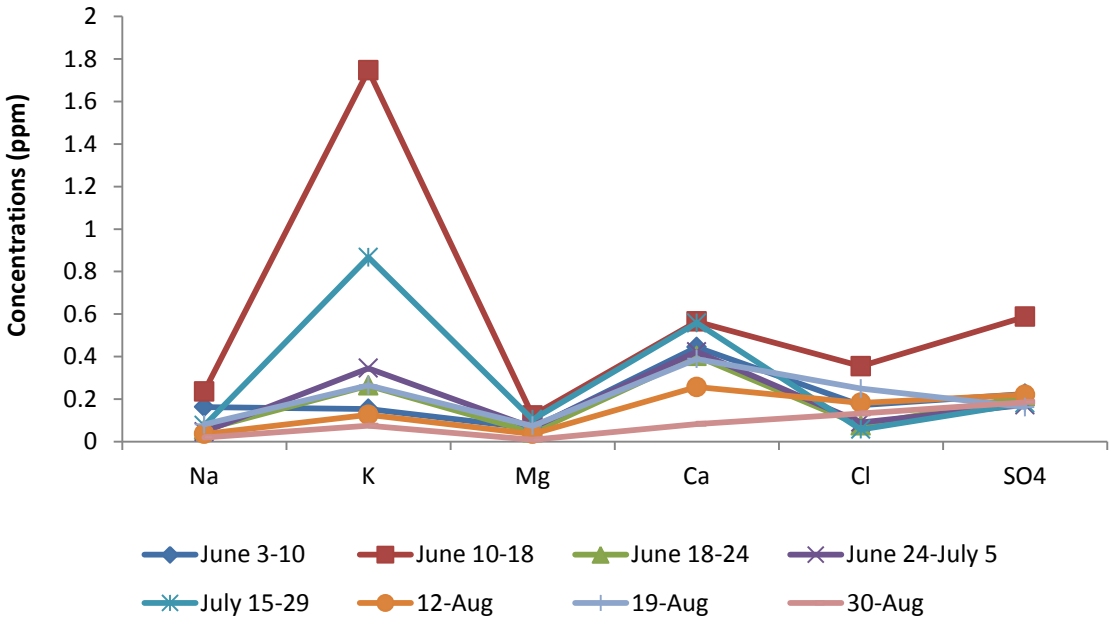

Figure 3.3 Schoeller diagram of precipitation geochemistry in Wolf Creek

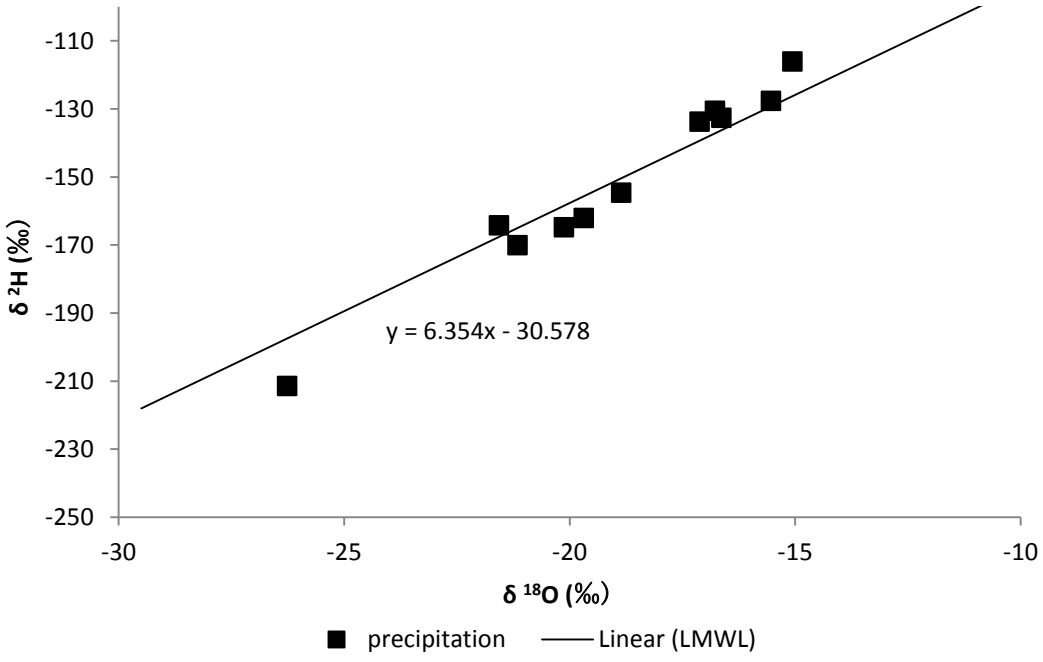

Figure 3.4 Oxygen and hydrogen stable isotopes of precipitation samples

3.3 Summer Water Sampling

The main objective for summer sampling was to find end-member water sources within Wolf Creek watershed. The geochemistry of summer water samples is illustrated in Figure 3.5, and shows variation related mixing of distinct water sources. All the samples had low TDS and neutral pH values.

Most samples were Ca-HCO_3 type of water while three of them are Ca-SO_4 type of water. The three Ca-SO_4 type water samples were taken from two quarry ponds and a lake. They were concentrated in all major ions including Cl^-, Na^+ and K^+. They were also enriched in heavy stable isotopes (Figure 3.6), a result of isotopic fractionation associated with evaporation (Clark and Fritz, 1997).

One of the water samples was obtained where a shallow spring discharged onto the ground at the foot of a hill. This sample represents soilwater comprising infiltrated meltwater and active layer thawed water that was driven downslope by gravity and rose through fissures in the soil. This sample was less concentrated in dissolved ions and depleted in heavy stable isotopes compared with the lakewater samples. But it contained much more dissolved ions than the precipitation samples collected in 2012. Reactions within soil horizons probably added dissolved ions to the soilwater. However, the depleted $\delta^{18}O$ and $\delta^{2}H$ values revealed its meteoric origin and short residence time in the ground.

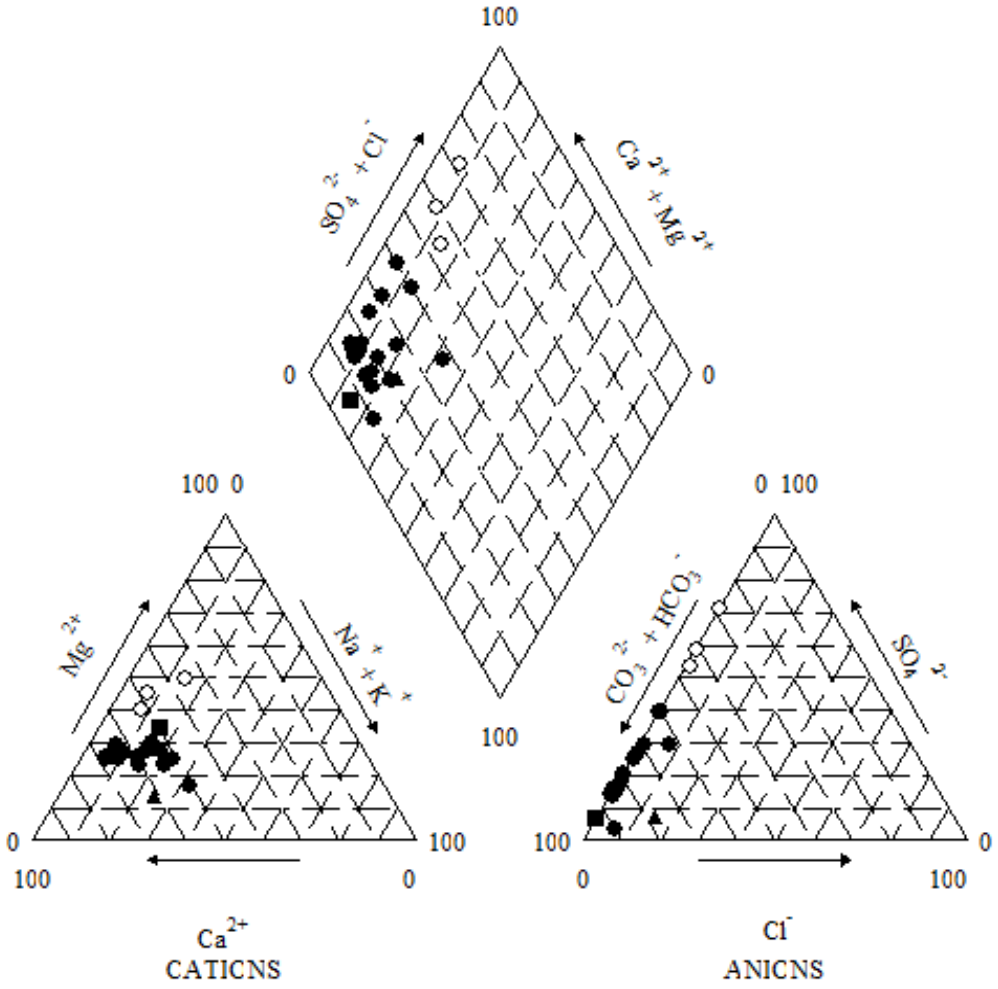

Figure 3.5 Piper diagram for the Wolf Creek summer sampling water samples (open circle: three Ca-SO_4 type water samples; square: soilwater; triangle: snow sample; solid circle: other water samples)

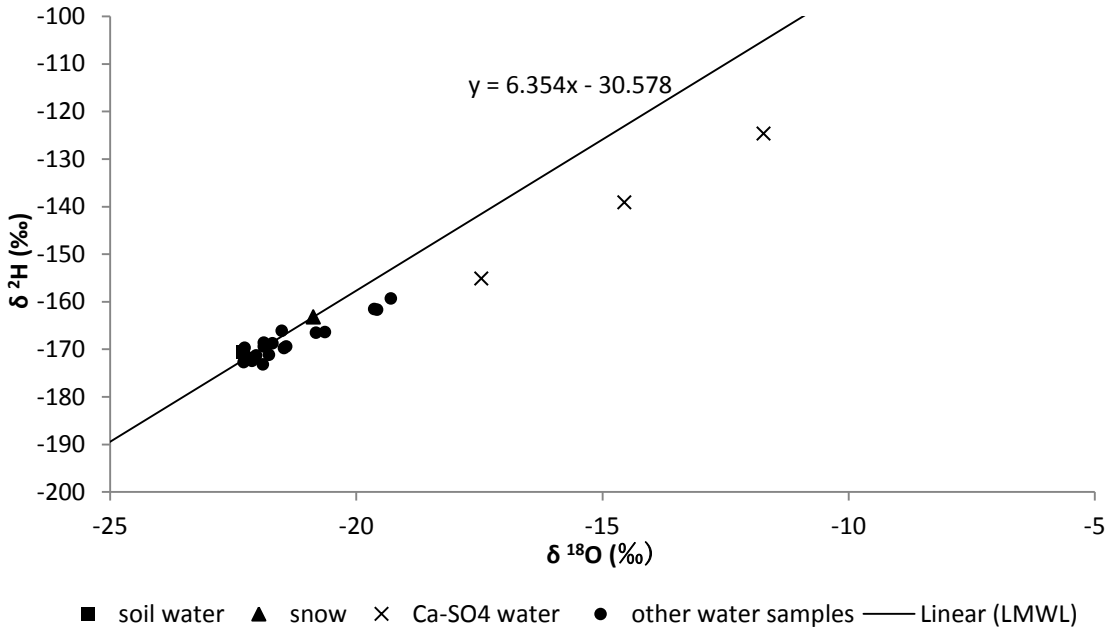

Figure 3.6 Oxygen and hydrogen stable isotopes of Wolf Creek summer sampling water samples.

3.4 Wolf Creek Streamwater

Samples from Wolf Creek were taken routinely every 7-10 days. These streamwater samples provided a chance to learn how the time series of geochemistry changed in spring and summer, including the melt season, which was the most influential hydrological event in such a sub-arctic watershed. Continuous discharge measurements were conducted and processed by the Water Resources Branch of Environment Yukon. The flow gauge was set up at Wolf Creek where it was accessible from the Alaska Highway, at the same place where streamwater samples were taken. Streamwater samples were collected and analyzed for geochemistry and isotopes.

3.4.1 Discharge

Wolf Creek was unfrozen from April 27th to October 16th in 2012. The discharge was measured during this period. The discharge varied considerably in Wolf Creek over the study period (Figure 3.7). Meltwater was added to the baseflow during the spring freshet. Precipitation also affected the streamflow because it generated runoff. There were three obvious increased flow events during the study period. They all happened before July. The first peak occurred on May 27th. The flow increased from 0.38 m^3/s on April 27st to 2.99 m^3/s on May 27th. The second and maximum peak in Wolf Creek discharge occurred on June 8th. The flow in the stream increased to 8.25m^3/s only in two weeks. The final peak came on June 22nd. After this peak, the streamwater began to retreat in July and maintained a flow rate around 1.2 m^3/s from August to mid-October.

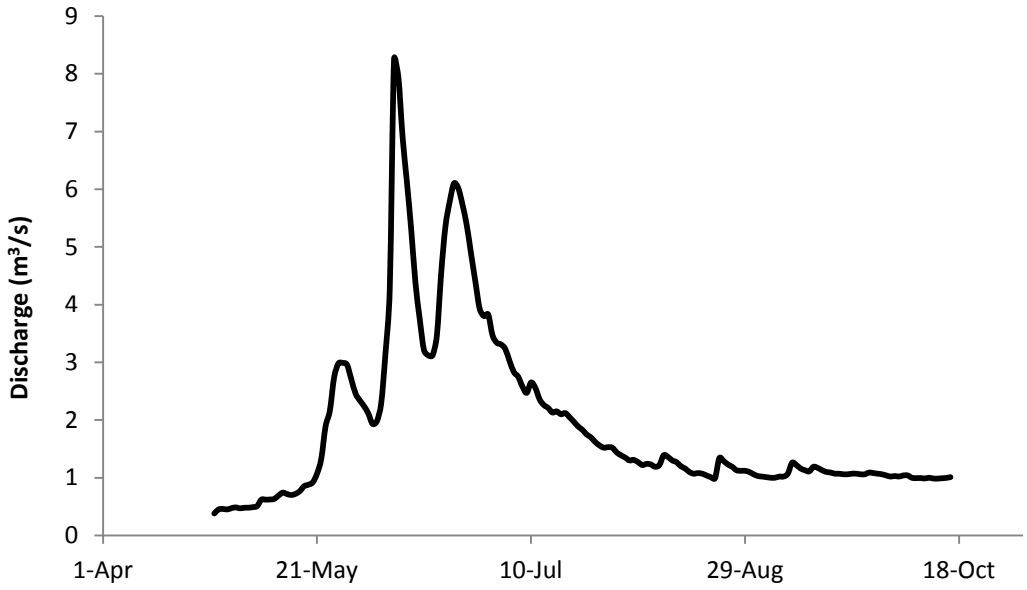

Figure 3.7 Discharge of Wolf Creek at the Alaska Highway from April 27th to October 16th

3.4.2 Major Ion Geochemistry of Wolf Creek Streamwater

Concentrations of major anions and cations, sodium (Na^+), calcium (Ca^{2+}), potassium (K^+), magnesium (Mg^{2+}), sulphate (SO_4^{2-}) and chloride (Cl^-) were above the detection limit in Wolf Creek streamwater samples. The streamwaters were more concentrated in dissolved ions than precipitation samples. Ions like Na^+, Ca^{2+}, Mg^{2+} and SO_4^{2-} are also present in deeper groundwater (Pinder and Jones, 1969; Langmuir, 1997; Boucher, 2009) where they are derived from interactions between groundwater and rocks and/or soils Time series plots of these ions in Figure 3.7 (a)-(d) indicate that streamwaters have the highest concentrations in April. A sharp decline occurs between the middle of May and early June when minimum values are recorded. Then concentrations partially recover through mid-September. In contrast, concentrations of K^+ and Cl^- had different time series (Figure 3.8 (e) and (f)). K^+ showed a rise during mid-May and then declined steadily to the end of the study period. K+ originated largely in organic soil horizon (Buttle and Sami, 1990; Boucher, 2009). Cl^- showed little variation over time with the exception of a single anomalously large value occurring in April.

Concentrations of weathering ions were inversely correlated with discharge rates (Figure 3.9 (a) to (d)). When meltwater or precipitation joined the stream, the groundwater was diluted by the two kinds of meteoric water, which were both depleted in all dissolved ions. The largest reduction of weathering ion concentrations were correlative with maximum streamwater discharge. In contrast, concentrations of K^+ and Cl^- had poor correlations with the discharge (Figure 3.9 (e) and (f)).

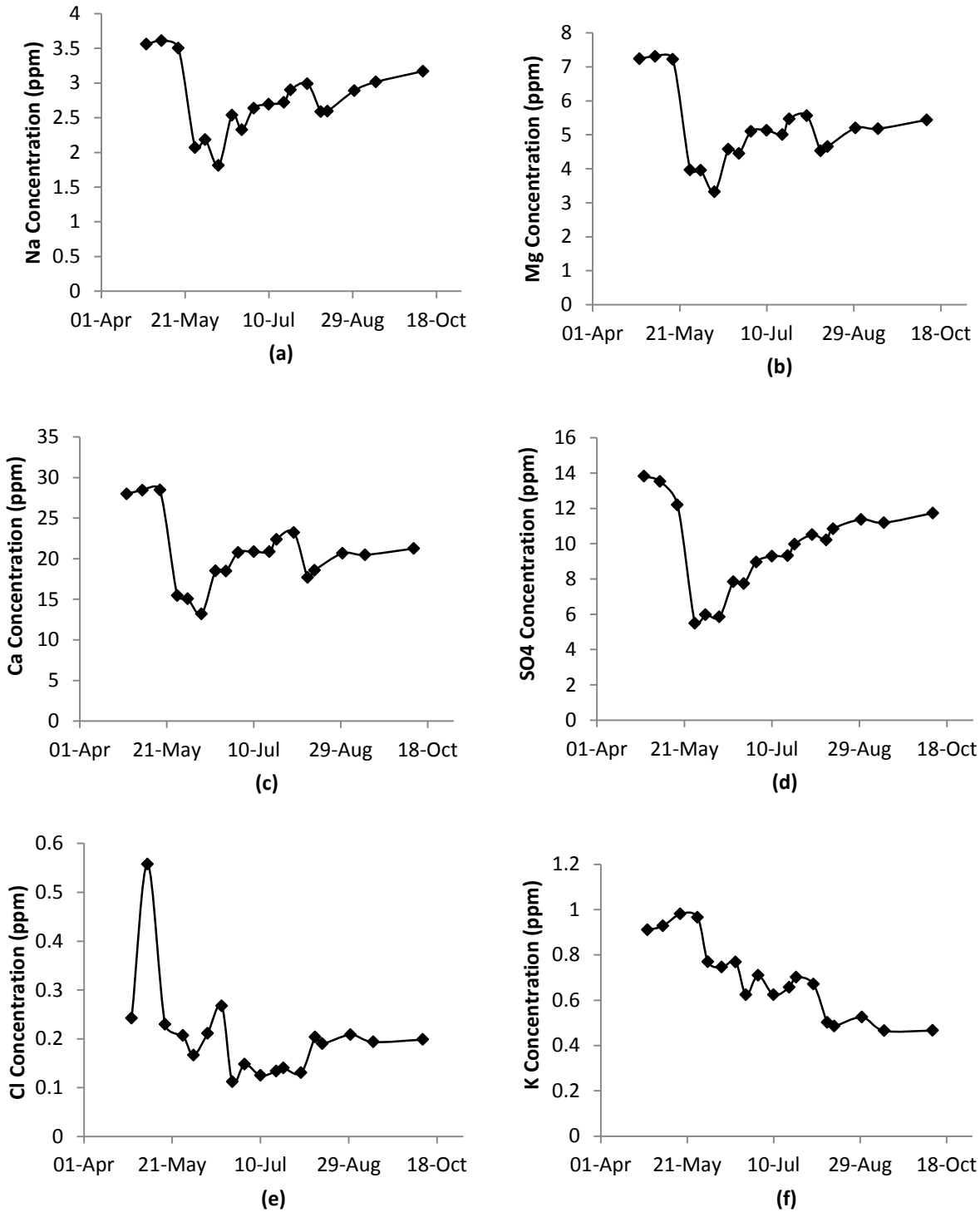

Figure 3.8 Time series of dissolved major ions in Wolf Creek streamwater from April 28th to October 10th, 2012, (a) Na^{+}, (b) Mg^{2+}, (c) Ca^{2+}, (d) SO_4^{2-}, (e) Cl^{-}, (f) K^{+}

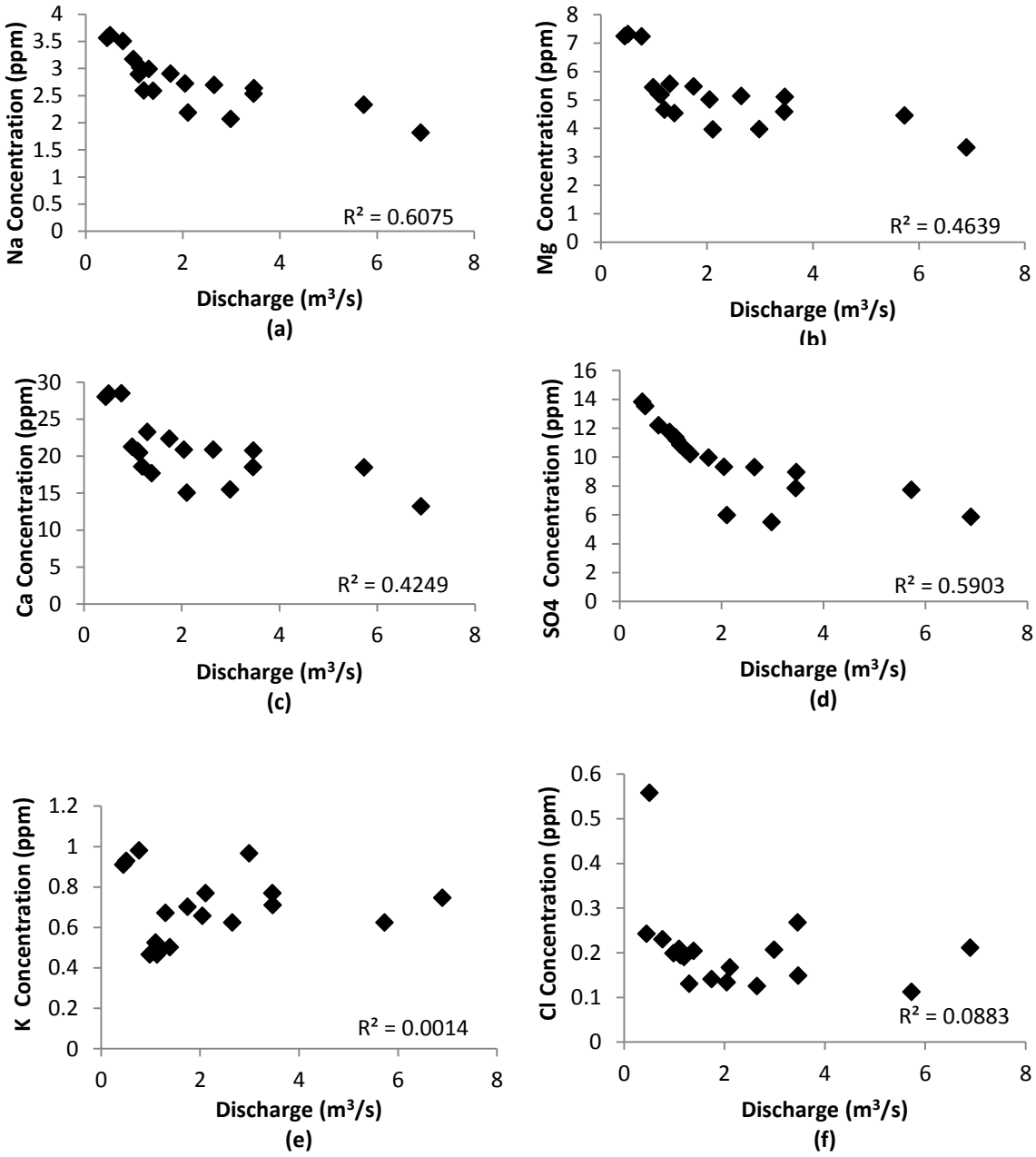

Figure 3.9 Major ion concentrations *vs.* discharge. (a) Na^{+}, (b) Mg^{2+}, (c) Ca^{2+}, (d) SO_4^{2-}, (e) K^{+}, (f) Cl^{-}

The concentrations of HCO_3^- were calculated according to the alkalinity values of each streamwater sample. The calculated HCO_3^- concentrations were higher than measured concentrations of other anions indicating that bicarbonate was the dominant anion in Wolf Creek streamwater samples. Ca^{2+} was as the dominant cation in streamwater.

A time series diagram of K:Ca ratios in Wolf Creek streamwater is shown in Figure 3.10. Aqueous molar solute ratios can provide additional information regarding to solute behaviour (Monteith et al, 2006; Boucher, 2009). The potassium concentration is biologically controlled while calcium concentrations are controlled by weathering processes. Thus high K: Ca ratios in streamwater indicate a large contribution from soilwater sourced in organic soils whereas low ratios represent more important contributions from groundwater sourced in the weathering horizon. The ratios in Wolf Creek were high from late-May to the end of June. Two peaks of K: Ca ratio occurred around May 27th and June 10th when the discharge was also high (Figure 3.10).

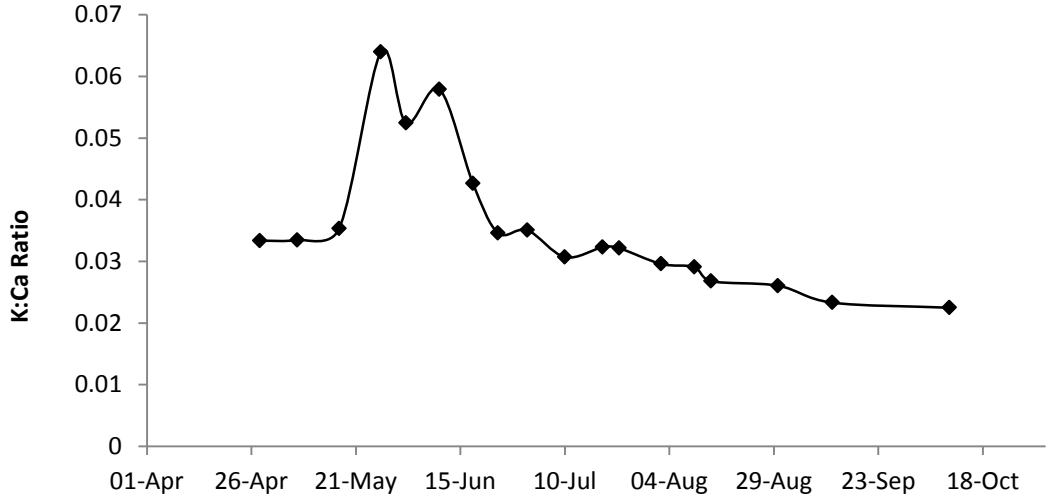

Figure 3.10 K: Ca ratios of Wolf Creek streamwater

3.4.3 Isotopes

3.4.3.1 Oxygen and hydrogen stable isotopes

The isotopic compositions of oxygen and hydrogen were determined for Wolf Creek streamwaters and compared with the local meteoric water line (LMWL) in Whitehorse as shown in Figure 3.11. Summer rains from July to October drove the $\delta^{18}O$ and $\delta^{2}H$ values of the streamwater toward the LMWL .

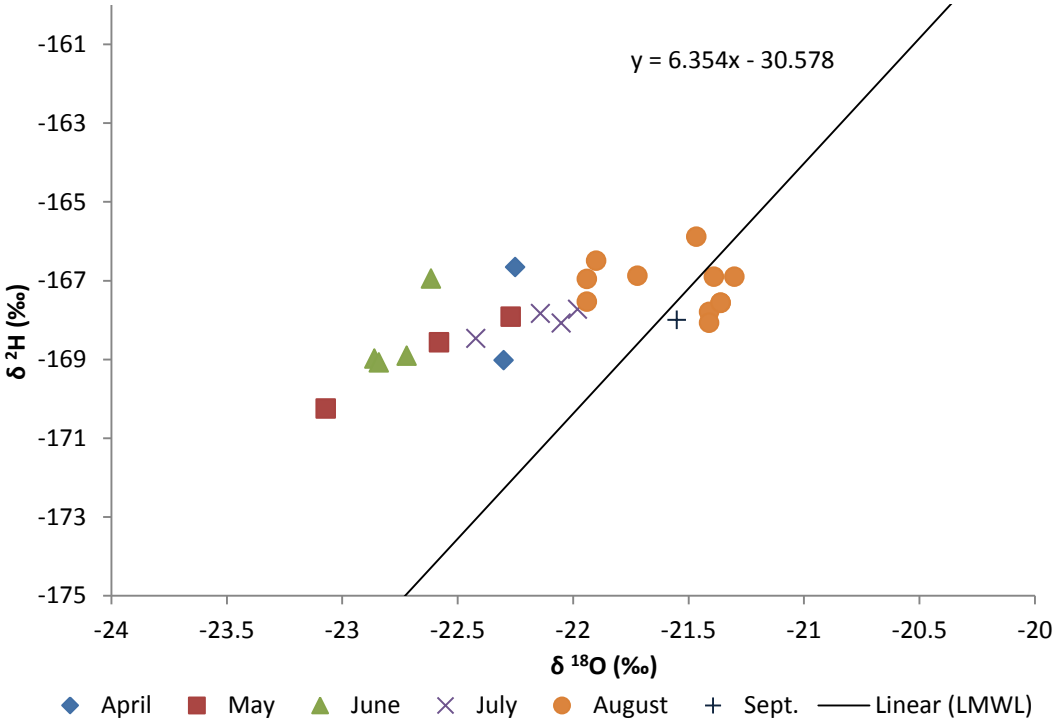

Figure 3.11 Oxygen and hydrogen stable isotopes of Wolf Creek streamwater

3.4.3.2 Tritium

Due to thermonuclear bomb tests, the average tritium concentration in precipitation was 4496 TU in Whitehorse in 1963 . In 1988 it was 22.417 TU, which is close to background levels.

A time series diagram of tritium concentrations and streamwater discharge from Wolf Creek is shown in Figure 3.12. Tritium concentrations were normalized to the concentrations the day samples were taken by correcting the analytical results based on the tritium decay function. All tritium concentrations were between 5 to 10 TU, which indicated less than 5 to 10 years residence time of modern water. The lowest concentrations occurred on May 27th, June 10th, June 24th and August 2nd, on which dates the highest discharges were observed. Peak concentrations occurred on June 2nd and 18th, coincident with the lowest discharge. Higher tritium concentrations indicated more young water joined the stream because of the short half-life of tritium. Residual tritium from the bomb test has disappeared in Wolf Creek and levels can be considered to be back to the natural background levels.

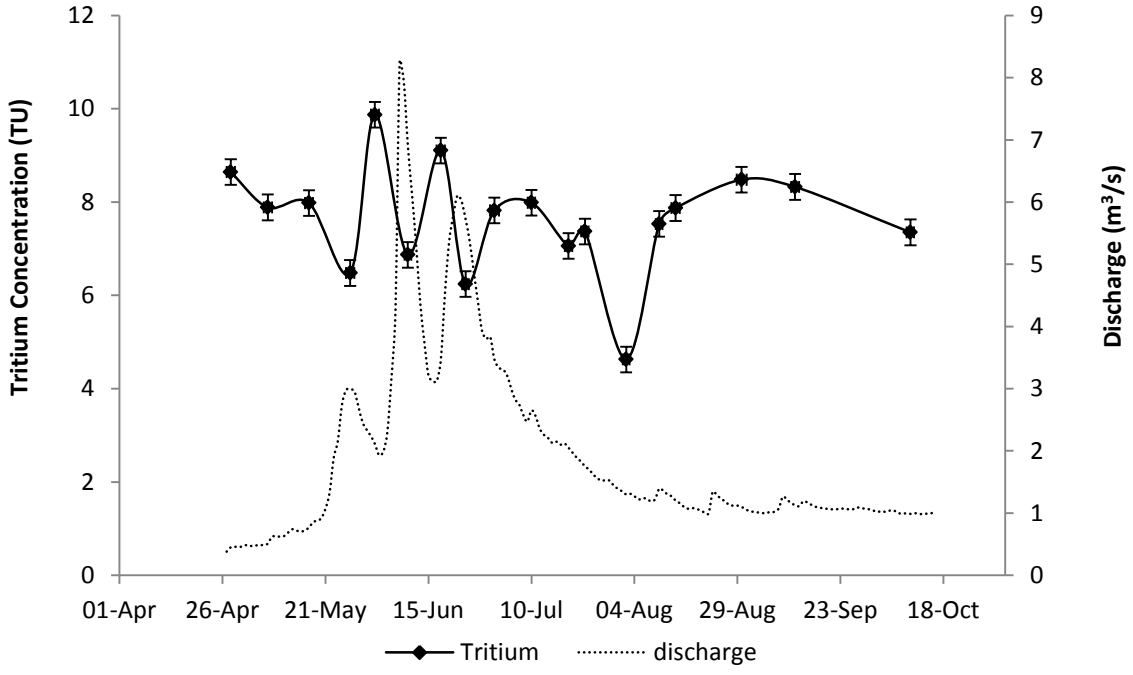

Figure 3.12 Time series of the tritium concentration and the discharge of Wolf Creek

3.4.3.3 Dissolved carbon, carbon isotopes and carbon export

Wolf Creek streamwater had an average pH value of 7.62 from April to October. The pH of water controls the carbon species (i.e., carbonic acid, carbon dioxide, bicarbonate and carbonate) comprising DIC (Clark and Fritz, 1997). Bicarbonate (HCO_3^-) was the dominant species of DIC in Wolf Creek streamwater although the concentration fluctuated in the time series. The time series of DIC concentration was similar with that of weathering ions (Figure 3.13). The concentrations of DIC decreased with the increased discharge.

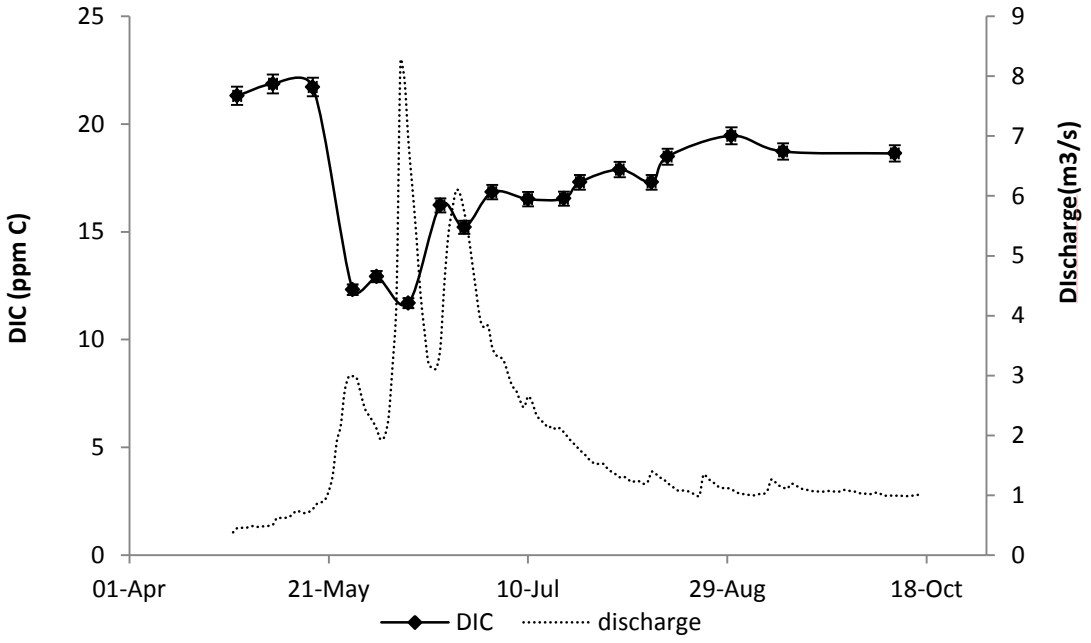

Figure 3.13 Time series of DIC concentration, unit: ppm C

Calcite saturation indices (SI) for streamwater were calculated with the software PhreeqC developed by the United States Geological Survey (USGS) and expressed in logarithmic scale. All calcite log SI values of the Wolf Creek streamwater indicated undersaturation with respect to calcite. The time series of calcite SI showed considerable variation throughout the study period (Figure 3.14). The calcite log SI values behaved the same way as weathering

ions like Ca^{2+}, and DIC, with initially high values decreasing rapidly to a minimum in June before recovering partially throughout the summer. Higher calcite log SI values are indicative of more dissolved calcite in streamwater, as observed in Wolf Creek before late-May. After late May, the calcite log SI values were lower which suggested less calcite dissolution and dilution by the meltwater and/or the precipitation inputs to the stream.

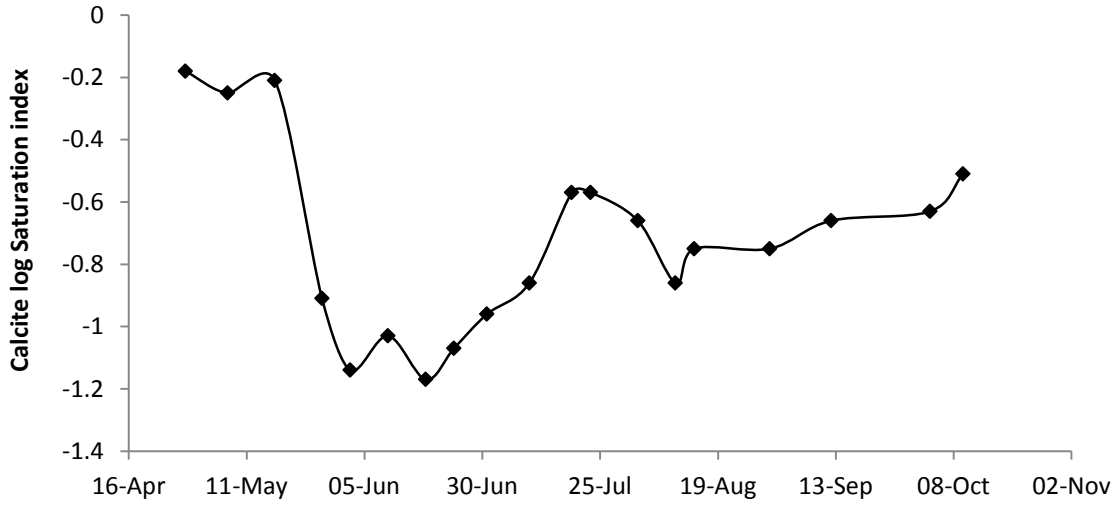

Figure 3.14 Time series of calcite logSI values of the Wolf Creek streamwater

Carbon isotopes in DIC can be used to determine the recharge conditions. The stable isotope ^{13}C is a good tracer for groundwater carbonate (Clark and Fritz, 1997). The $\delta^{13}C_{DIC}$ in Wolf Creek streamwater was relatively high in the baseflow and relatively low during the spring melt. The time series of $\delta^{13}C_{DIC}$ was similar to the time series of weathering ions, DIC and calcite log SI values (Figure 3.15). Streamwater samples taken before mid-May contained relatively high concentrations of dissolved. $\delta^{13}C_{DIC}$ values declined to a minimum from late-May to mid-July before returning to elevated values. The highest $\delta^{13}C_{DIC}$ values were recorded near the end of the study period.

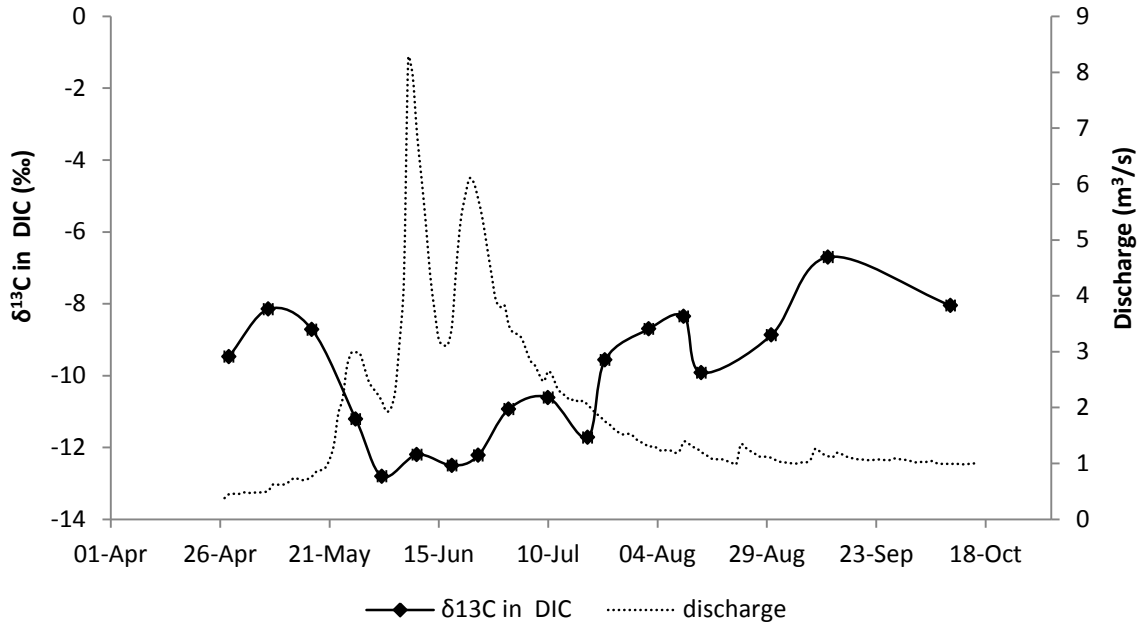

Figure 3.15 Time series of $\delta^{13}C$ in DIC of the Wolf Creek streamwater

The time series of $\Delta^{14}C$ is graphed in Figure 3.16, which exhibited trends similar to that of $\delta^{13}C$. High $\Delta^{14}C$ values occurred before June and after July when the discharge was low. The lowest $\Delta^{14}C$ values occurred during peak discharges in June. The dilution effect on $\Delta^{14}C$ from the discharge is clearly seen when $\Delta^{14}C$ values were plotted against the discharge (Figure 3.17). $\Delta^{14}C$ was depleted by the increased discharge from ~ -90‰ in the early May to -200‰ ~- 400‰ in June.

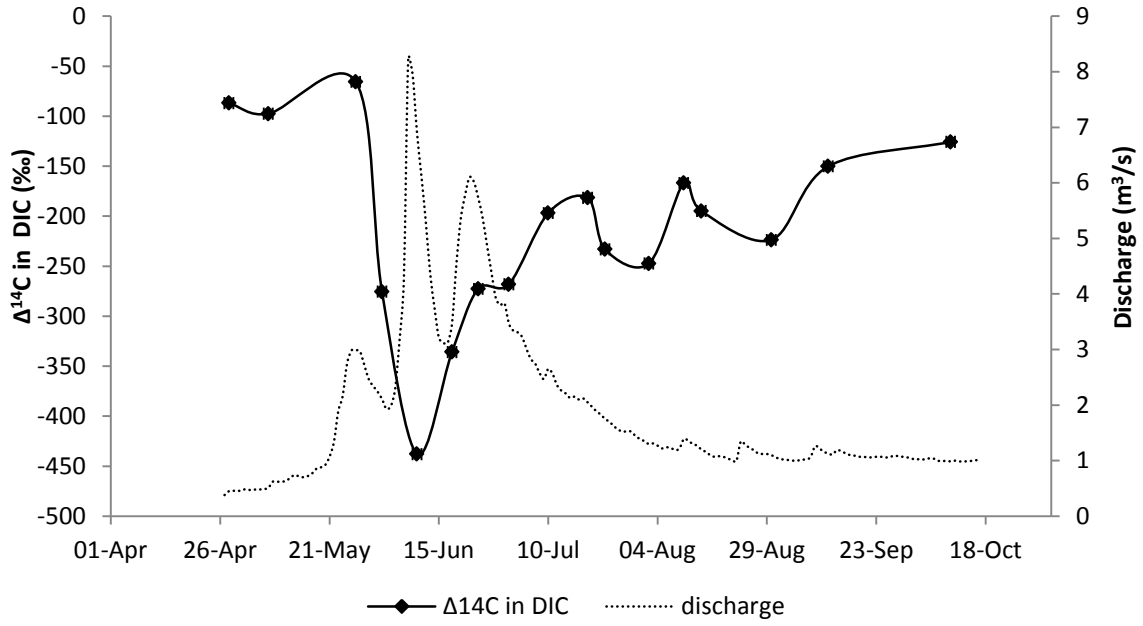

Figure 3.16 Time series of $\Delta^{14}C$ in DIC of the Wolf Creek streamwater

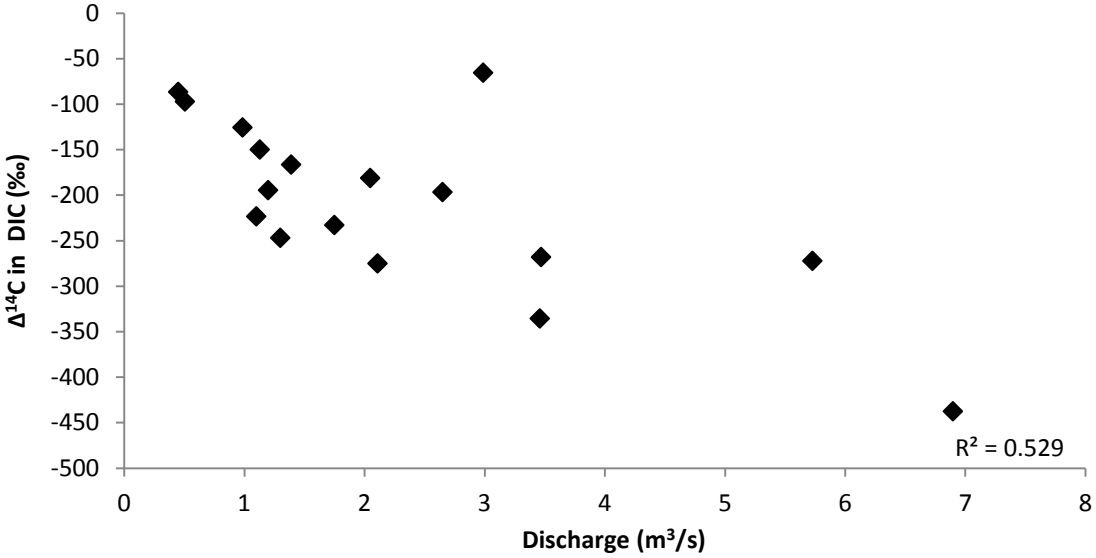

Figure 3.17 $\Delta^{14}C$ *vs.* discharge of the Wolf Creek streamwater

Most samples have P_{CO_2} values of 10^{-3} atm. P_{CO_2} values of 10^{-2} atm indicates open recharge

systems and 10^{-4} atm indicates closed systems. P_{CO_2}values of 10^{-3} atm are suggestive of a partially closed recharge system. The Percent Modern Carbon (pMC) values were also provided in radiocarbon dataset. The initial ^{14}C activity of open and closed systems are from 54 to 84 pMC respectively (Geyh, 2000). The pMC values of the Wolf Creek streamwater ranged between 50 to 100, which indicated a system that varied between open and closed conditions.

The dissolved inorganic carbon flux was calculated as the product of the DIC concentration and the discharge. During the study period, the discharge increased from 0.45 to 6.9 m^3/s, while the DIC flux increased from 9.6 to 87.2 g C/s. The time series of the DIC flux also showed a good correlation with the discharge, with peaks in the two being roughly coincident (Figure 3.18). DIC began with a flux of 9.6 g C/s in late-April. The DIC flux began increasing in mid-May and then dropped off again in July. From August, the DIC flux kept at a relative and constant level of 20 g C/s.

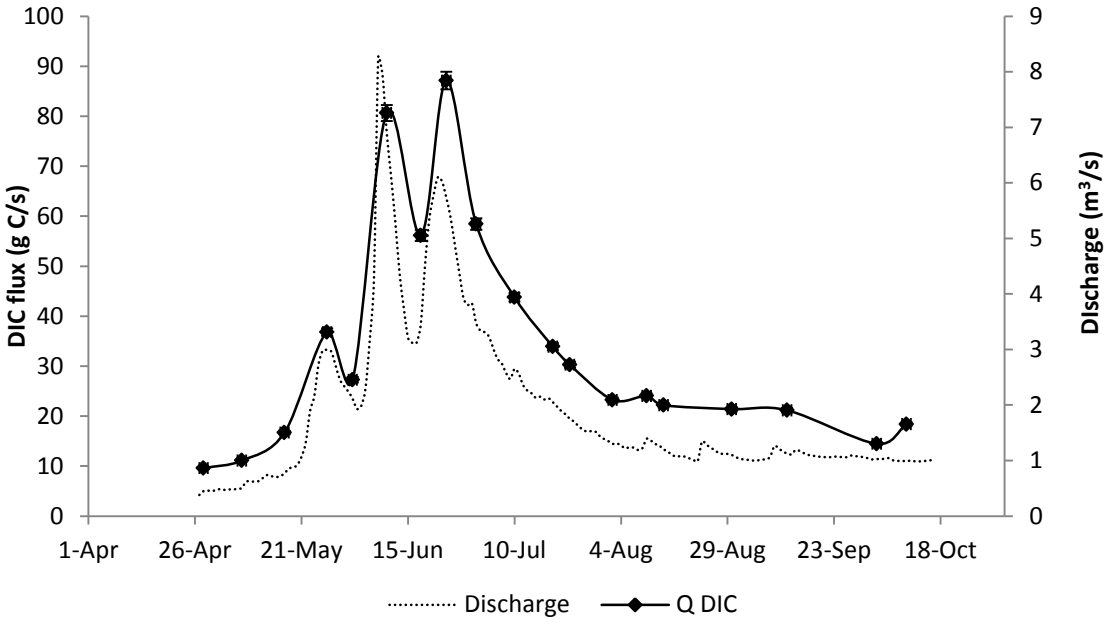

Figure 3.18 Time series of DIC flux and discharge of the Wolf Creek streamwater

DOC concentrations in the Wolf Creek streamwater ranged from 2 to 8 ppm C. They showed poor correlation with the discharge (Figure 3.19). The DOC flux was also calculated as the product of DOC concentration and the discharge. Maximum DOC export occurred during the high-discharge period (Figure 3.20). However, the DOC flux was lower than the DIC flux in Wolf Creek Research Basin during the study period. DIC constituted 70%-90% and DOC provided 10%-30% of the total flux of dissolved carbon via the landscape into Wolf Creek.

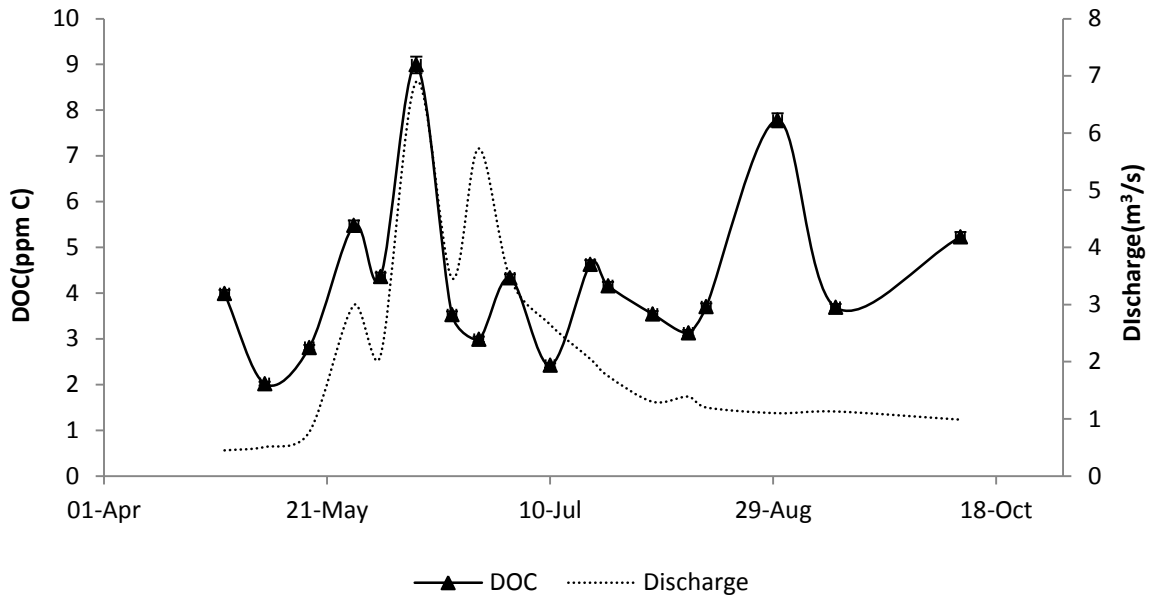

Figure 3.19 Time series of DOC and discharge of the Wolf Creek Streamwater

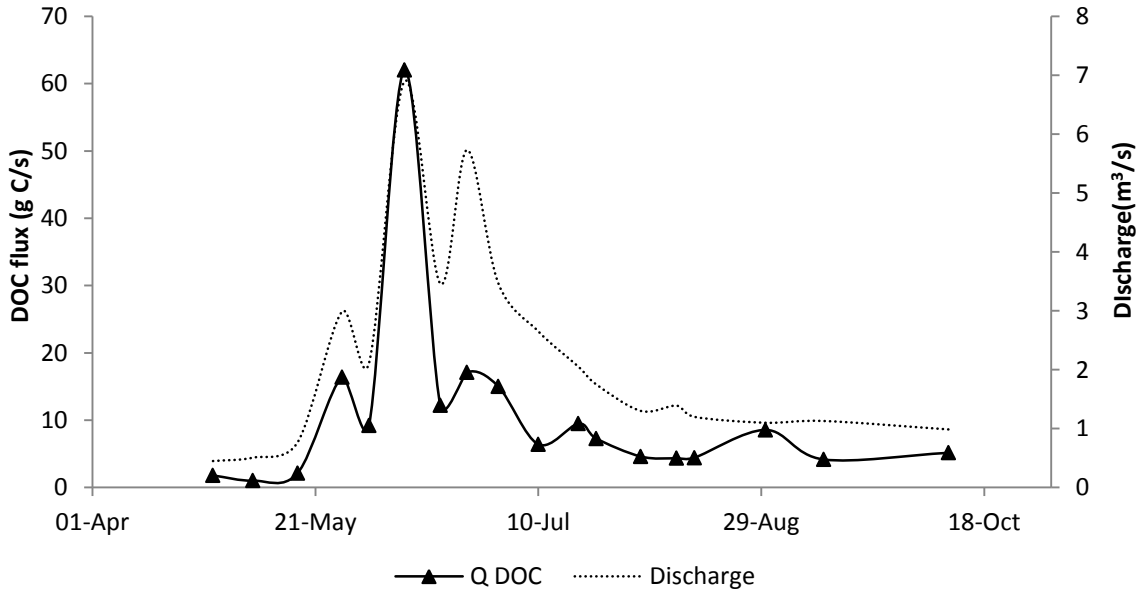

Figure 3.20 Time series of DOC flux and discharge of the Wolf Creek streamwater

3.5 Hydrograph Separation Results

Three end-members to Wolf Creek streamwater were identified based on the geochemistry and isotope chemistry of the water samples. As a result, a three-component hydrograph separation can be constructed for Wolf Creek. Because streamwater samples were taken weekly or bi-weekly, the hydrograph separation results mainly focus on the variations and trends of the contributions from each end-member, not the exact date.

The first component is the baseflow, which continues year round in Wolf Creek. The baseflow is the part of streamwater supported by groundwater. The baseflow contains elevated salinities and dissolved ions due to its long residence time in the zone of weathering beneath the surface. The streamwater before the snowmelt (April) is considered to be most representative of the baseflow. Another component is the soilwater discharge, which is a mixture of infiltration water and seasonal frost drainage through the soil to the stream. This water is of meteoric origin, less concentrated in dissolved ions compared to groundwater because of its reduced residence time underground. One of the summer samples was a direct measurement of soilwater. The last component is precipitation runoff. Precipitation samples also showed the least concentrated geochemistry. Both the precipitation and soilwater had low dissolved ions, so they diluted the baseflow when they joined the stream. Part of the geochemical data of all three components is listed in Table 3.1.

Table 3.1 Geochemistry of each end-member used for hydrograph separation

Sample	Ca^{2+} (ppm)	SO_4^{2-} (ppm)	DIC (ppm C)	$\delta^{18}O$ (VSMOW,‰)	$\delta^{2}H$ (VSMOW,‰)
Baseflow	28.29	13.18	21.63	-22.37	-167.72
Precipitation	0.37	0.25	0.94	-18.72	-150.42
Soilwater	7.92	1.71	9.1	-22.3	-170.62

End-member mixing diagrams of several tracers were plotted to assess the quality of the hydrograph separation. In cases where the stream composition at a peak flow defined a point in the triangle representing the end-members on a mixing diagram, three-component hydrograph separation was possible. For any diagram producing a successful separation, it was noted whether or not the streamwater sample fell within the confined triangle of the three end members. If so, the result was recorded as "good". If the streamwater value did not fall within the triangle formed by the three end-members, the result was recorded as "poor". If the streamwater value fell on or just outside of one of the borders of the triangle, approximately within the analytical error for the tracers, the result was recorded "good/poor" (Rice and Hornberger, 1998). The mixing diagram based on Ca^{2+} and $\delta^{2}H$ (Figure 3.21) provided the best separation of end-members and generally a "good" quality of mixing. Therefore the remainder of the hydrograph separation analysis is based on these two tracers.

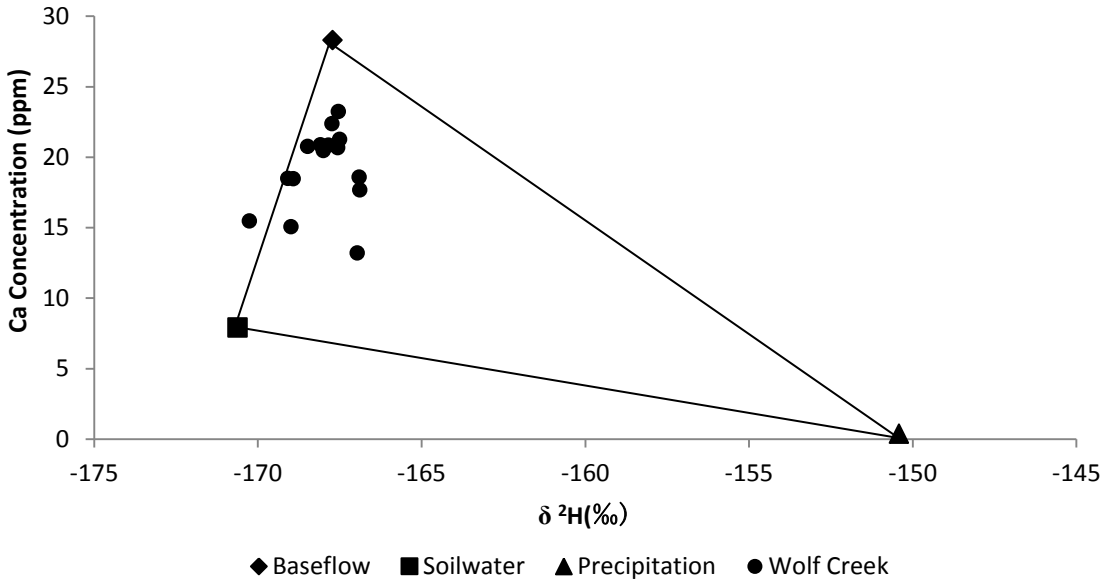

Figure 3.21 Mixing diagram for the Wolf Creek streamwater using Ca^{2+} and δ^2H as tracers

The relative importance of each component in the total stream flux was expressed as Qgw/Qt, Qp/Qt and Qs/Qt and plotted as time series in Figure 3.22. The baseflow supported over 98% of the streamwater before mid-May. Soilwater started to enter the stream in mid-May and its discharge accounted for more than 50% of the streamwater from mid-May to mid-June, which accounted for the bulk of the melt season. For the rest of the time, the baseflow once again became the major contributor to the Wolf Creek streamwater. The contribution from the precipitation was always relatively low.

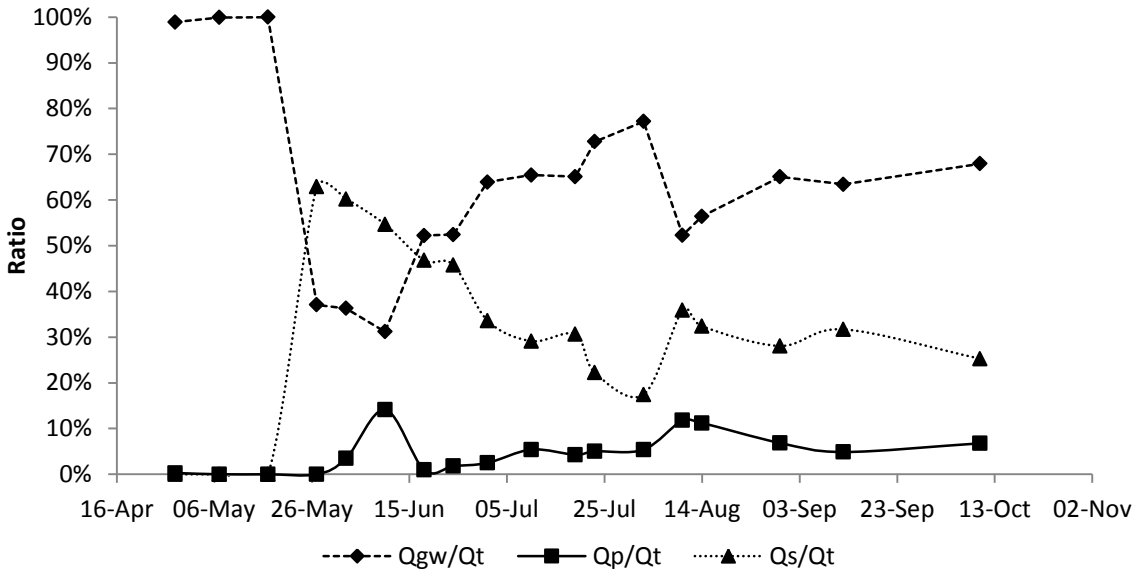

Figure 3.22 Hydrograph separation results for relative contribution of each end-member compared to the total flux in Wolf Creek

The spring freshet in Wolf Creek was punctuated by three major episodes that occurred around May 27th, June 10th and June 24th. The hydrograph separation in Figure 3.23 records a unique end-member signature for each episode. Precipitation was generally a minor contributor to the streamflow suggesting that low contribution from direct precipitation. From the beginning of mid-May to mid-June, soilwater was the major contributor to the freshet. During the rest time in the study period, baseflow discharge dominant the hydrograph. Throughout the melt event groundwater discharge to the creek increased steadily. Between mid-May and late June, the melt kept expanding and delivering soilwater to the stream. When most soilwater had reached Wolf Creek, a falling off came thereafter.

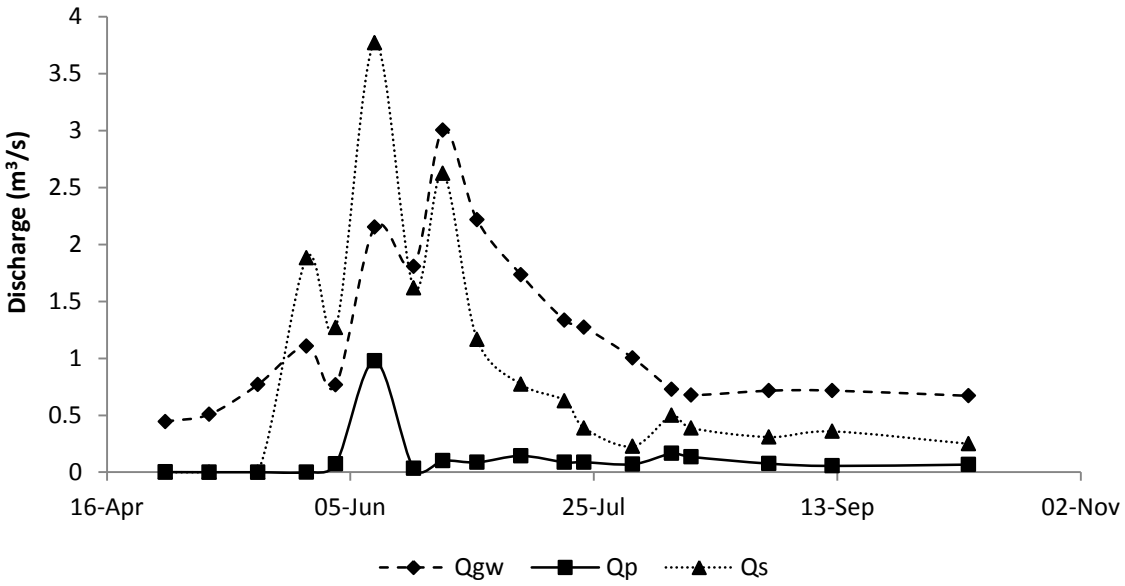

Figure 3.23 Hydrograph separation results for discharge of each end-member in Wolf Creek

4. Discussion

The goals of this thesis were to: (1) study the temporal variations of geochemical tracers in streamwater and groundwater, (2) understand the contributions from each end-member, especially the groundwater component, to the catchment, (3) examine seasonal variations of composition, discharge and carbon export in streamwater and groundwater. This chapter provides a discussion of results of this work.

4.1 Hydrograph Separation and Runoff Process

The three-component hydrograph separation technique separates the soilwater and the groundwater as two distinct components, both representing water stored beneath the ground surface (McNamara *et al*., 1997; Dewalle *et al*., 1988). Because of the challenges of sampling groundwater directly, it is commonly assumed that stream baseflow is representative of the groundwater (McNamara *et al*., 1997). .

The hydrograph separation results showed that baseflow made up at least 30% of streamwater from April to October in 2012. Only during the period of melt from late-May to the end of June, soilwater dominated the Wolf Creek streamwater. The melt started around May 17th in spring, as evidenced by a surge in the soilwater discharge. Three soilwater discharge peaks were observed during the study period. The melt kept expanding until June 10th when most of the soilwater had been delivered to the stream. After June 10th, the spring melt began to retreat. However around June 24th, due to the rising temperature in summer, there was a final pulse of meltwater that contained both soilwater and groundwater contributions. During the peak

freshet of streamwater, the stream flow was dominated by the soilwater from the organic layer. The proportion of the soilwater contributing to the streamwater declined, however, as seasonal frost thawed, mixing with and being displaced by infiltrated meltwater (Carey and Quinton, 2004). Variations in soilwater discharge were related to the degree of snowmelt in Wolf Creek.

At the beginning of the melt, the meltwater percolating from the snowpack infiltrates the ground, which is typically unsaturated (Carey and Quinton, 2004; Carey *et al.*, 2013; Quinton *et al*., 2005; McCartney *et al.*, 2006). For the ground underlain by the permafrost, the infiltration is mainly restricted to the porous organic soil, whereas in the ground with seasonal frost, percolation is uninhibited unless there are ice-rich layers at depth (Kane and Stein, 1983). During this early stage of the melt, there is little transfer of water to the stream until unsaturated storage capacity is satisfied and the infiltrating meltwater supplies sensible heat to bring the soil to 0℃(Carey *et al.*, 2013; Carey and Quinton, 2004). At this time, the soilwater runoff is rapidly transferred to the stream via lateral runoff through the organic layer

Several precipitation events were recorded during the study period although the contribution to the Wolf Creek discharge from the precipitation was low. Intensive and heavy precipitation occurred from late-June to September, this was the reason for relatively higher contribution of the precipitation from June to September. Precipitation may infiltrate into the ground and become a part of the soilwater or groundwater that would recharge the Wolf Creek streamflow. The infiltration and transfer process takes time, depending on the hydrogeological setting within the field. However, as the melt happened mainly between mid-May to late-June, the meltwater probably saturated the near-surface soil. Precipitation may not have been able to

infiltrate into the ground and would instead have generated overland runoff to reach the stream directly.

An assumption usually implied but not explicitly stated for hydrograph separation is that the groundwater reservoir maintains a stable isotopic and chemical composition year round (Rice and Hornberger, 1998). The near-stream shallow groundwater supplies the stream baseflow. It can be easily affected by surface water infiltration. During the peak melt, high discharge from the groundwater was also observed around June 10th and 24th. This could be the result of increased groundwater recharge caused by soilwater infiltration and/or reflect thawing in the active layer down to the groundwater. The baseflow was highly diluted by the soilwater component within several days in mid May. But the streamwater discharge took several months to recede after the melt. At the end of melt, the soilwater and precipitation may have continued infiltration and mixing with the subsurface water, including groundwater from the mineral weathering zone, leading to the dilution and displacement of groundwater, involving processes identified by Carey and Quinton (2004). The melt discharge time series produced a sudden rising limb reflecting increases in discharge due to diurnal snowmelt cycles and precipitation events, and a longer recession limb . This primary pattern was punctuated by three discharge pulses or events, but the cause of the pulses are unclear.

Contribution of precipitation may link to the overland flow of rainfall and snowmelt. Precipitation can also infiltrate, bring heat to thaw the permafrost and recharge the groundwater as well. The infiltration can transfer the heat to the permafrost and cause it to thaw. Deeper flow paths will be expanded as a consequence, and weathering will be enhanced and more groundwater will be delivered to the surface.

4.2 Geochemistry and Isotopes of the Wolf Creek Streamwater

4.2.1 Geochemistry

Water in the stream has a baseflow component all year round if it does not dry up in the winter. However, streams typically have more than one recharge source and recharge sources themselves will have seasonal variations. Water from distinct recharge sources will bring distinct geochemistry into the stream and also cause variations in streamwater geochemistry (e.g. dissolved ion and isotope concentrations). Soilwater and precipitation contain few dissolved ions. Baseflow is sourced in groundwater having a long residence time in bedrock and/or soil, which contribute abundant dissolved ions. In this study, high concentrations of ions like Ca^{2+}, Mg^{2+}, Na^{+} and SO_4^{2-} are supplied by the baseflow. The baseflow would be diluted by soilwater and precipitation contributions to Wolf Creek.

In Wolf Creek, dilution of weathering ions contained in the baseflow occurred suddenly in mid-May as a result of the melt and continued until mid-June. Although weathering ion concentrations increased after that, they failed to return to the high levels of the pre-melt baseflow. This may be due to minor soilwater and precipitation joining in the stream, or a redefined baseflow composition that characterizes late summer baseflow, and that may evolve over the freeze-up period. Soilwater and/or precipitation were responsible for the dilution events in the stream. However, as mentioned before, the recharge of groundwater from the soilwater and/or the precipitation may happen during the study period, which could be another reason for the less concentrated streamwater. DIC and calcite SI had time series similar to those of the weathering ions, because they were all derived from the weathering zone. Cl^{-} is

highly soluble and conservative so that its concentration is similar across the watershed (Petrone *et al.*, 2006). Coal outcrops were discovered in upstream on the Mount Granger and the Coal Lake of Wolf Creek Research Basin in 1990 (Hill, 1982), and may have contributed to SO_4^{2-} in the streamwater. However, Na^+, Cl^- and SO_4^{2-} also originate from organic soils and accumulate via evaportranspiration and organic decomposition (Boucher, 2010). K^+ has less mobility and can easily be absorbed by organic matter.

Based on the understanding that potassium is mainly derived from vegetation and calcium from the weathering zone (Elsenbeer *et al.*, 1995), K: Ca ratios can be used to distinguish the streamwater components and pathways. High K: Ca ratios suggest fast and near-surface pathways interacting with the biological system. Low K: Ca ratios indicate slow and deep pathways of groundwater circulation and weathering. High ratios occurred within Wolf Creek melt period indicating rapid, near-surface runoff of the soilwater. Before and after the melt, K: Ca ratios were relatively low indicating the dominant contributions of groundwater and deeper flow paths.

4.2.2 Isotopes

The isotopes of water, ^{18}O and ^{2}H, are depleted in the Wolf Creek streamwater compared to the summer precipitation samples collected in Whitehorse, as streamwater $\delta^{18}O$ and $\delta^{2}H$ values were plotted on the left side of the local meteoric water line (LMWL). Depletion of $\delta\ ^{18}O$ was especially noteworthy. The reason for this phenomenon is relate to the direct infiltration and isotope exchange of meltwater through the snowpack which transferred into the stream in spring melt, as the depletion was more obvious during May and June. Continuous exchange

between the meltwater and snow would cause a Rayleigh-like enrichment of the meltwater (Clark and Fritz, 1997). Although isotopic fractionation processes operating during meltwater formation and snowpack sublimation can be calculated using the same equilibrium fractionation factors to yield similar trends in Figure 4.1 (Clark and Fritz 1997), they are two distinct processes. The first meltwater to exit from the snowpack is highly depleted and plots above the meteoric water line (Clark and Fritz, 1997). Another possible explanation for the depletion of isotopes in the Wolf Creek streamwater, could be the Aleutian Low commonly occurring in winter in North America. A strong Aleutian Low and its eastward movement could possibly enhance Rayleigh distillation and cause isotopic depletion in precipitation (Anderson, 2005).

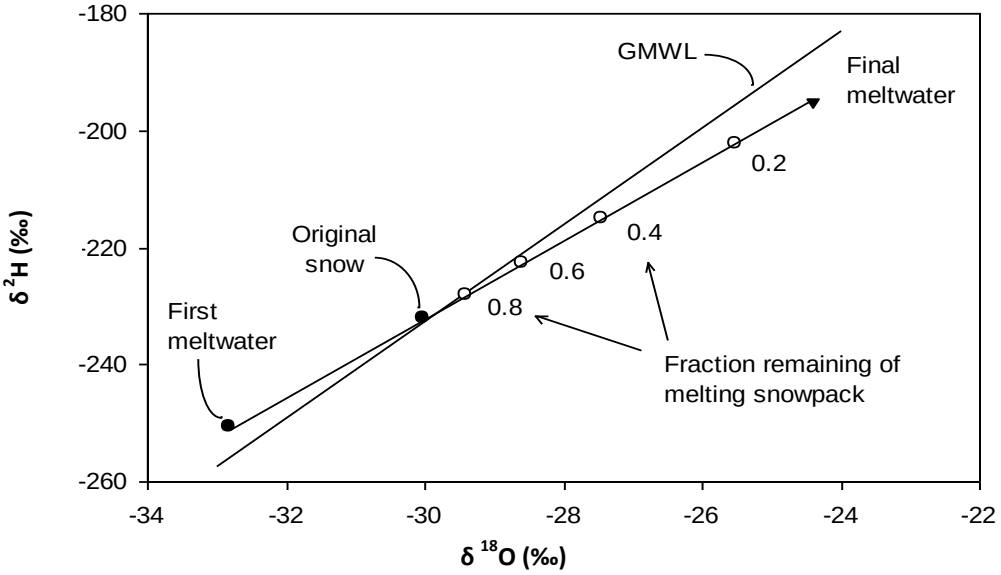

Figure 4.1 Theoretical evolution of isotopes in meltwater draining from base of snowpack, based on complete equilibrium between the water and the snowpack (Lauriol *et al.*, 1995, Clark and Fritz, 1997)

The tritium concentrations in the Wolf Creek streamwater correlated negatively with discharge from late-May to the beginning of July. When the discharge was high, the tritium concentration was low. Furthermore tritium values of Wolf Creek baseflow indicate a relatively short residence time of groundwater in local reservoirs. Precipitation delivers tritium to the hydrological system by infiltration and recharged the soilwater or the deep groundwater. In general, water stored in the ground has relatively longer residence time, in which tritium decay occurs, thus reducing the tritium concentration. However, there was no big difference in tritium concentration (like >10 TU) in the streamwater of Wolf Creek from late April to mid- October. This provides evidence that Wolf Creek Research Basin has a fast-moving hydrogeological system, and that the baseflow experienced a relatively short residence time (<10 years), so that most tritium in precipitation can be transferred into the stream.

4.3 Carbon Isotopes and Carbon Export

Based on the hydrograph separation, the DIC flux was highly synchronous with the baseflow (Figure 4.2) At least two DIC reservoirs were indicated. One is the baseflow and another one is the freshet during the melt. The streamwater in Wolf Creek started and ended the time series with water enriched in ^{13}C and ^{14}C, reflecting isotopic enrichment typical of groundwater. During the melt, the streamwater was diluted by isotopically depleted soilwater

and became depleted in carbon isotopes, ^{14}C (Figure 3.16) and $\delta^{13}C$ (Figure 3.15). The shifts in DIC, $\Delta^{14}C_{DIC}$ and $\delta^{13}C_{DIC}$ over the melt season reflect changes in the source of DIC exported from the catchment. The $\Delta^{14}C_{DIC}$ and $\delta^{13}C_{DIC}$ were plotted together in Figure 4.3 The processes that will dilute radiocarbon in DIC with dead carbon include carbonate mineral dissolution (calcite, dolomite) in recharge areas and oxidation of old organic matter along flow paths or within the aquifer etc. (Clark and Fritz, 1997). The dead carbon may also come from thawing permafrost via newly developed deep flow paths. However, the exact dead carbon source cannot be identified from the Figure 4-3.

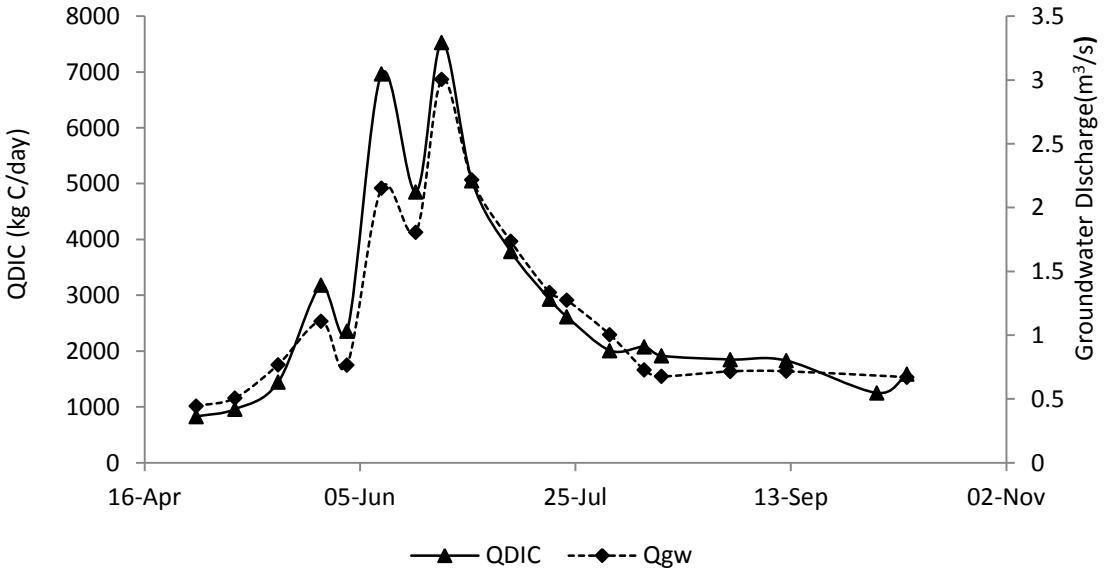

Figure 4.2 Time series the DIC flux and the baseflow discharge

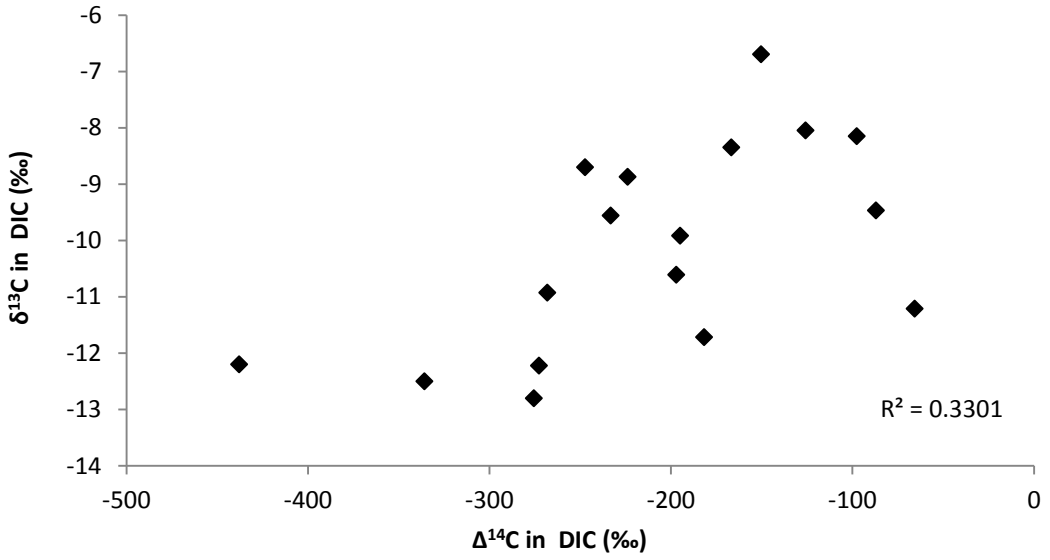

Figure 4.3 $\Delta^{14}C$ *vs.* $\delta^{13}C$ of streamwater in Wolf Creek

DIC concentrations and DIC export were inversely correlated in the Wolf Creek time series. The concentrations of DIC in Wolf Creek peaked when the groundwater was at its highest flows, and decreased as the proportion of groundwater component decreased. Maximum DIC flux occurred during the melt season, while DIC concentration dropped markedly in that period. The high total discharge was responsible for the export of DIC. Deeper infiltration and enhanced weathering probably delivered more DIC to the stream by thawing permafrost (Hinzman *et al.*, 2005; Lyon *et al.*, 2010). A generally increasing trend in the groundwater contribution has been identified across the Yukon River Basin as a result of changed hydrological flow paths due to permafrost thawing, and this alternation of flow paths is believed to further increase the DIC export (Walvoord and Striegl, 2007; Lyon and Destouni, 2010; Lyon *et al.*, 2010).

The concentration of DOC correlated inversely with discharge but the correlation was weak.

In Wolf Creek, the peak DOC export was on June 10th when the melt was also at its peak. The peak DOC concentrations coincided with the snowmelt and summer storms (Petrone *et al.*, 2006), which was opposite to the behavior of DIC. The DOC transport in streams is an important pathway for carbon loss from terrestrial ecosystem (Balcarczyk *et al.*, 2009). However, the DOC flux prior to and after the melt was much lower. In areas underlain by permafrost, flow is largely restricted to organic horizons and leaches DOC from the soil (Balcarczyk *et al.*, 2009). In low permafrost-coverage areas, flow can infiltrate into deeper organic layers and mineral layers where DOC absorption and weathering occur (Balcarczyk *et al*., 2009; Petrone *et al.*, 2006). Increased flow paths, residence time and microbial mineralization in the active layer and groundwater will decrease the DOC export (Striegl *et al*., 2005). So the effect of permafrost on the hydrogeology of Wolf Creek Research Basin is evident in the DOC results.

In Wolf Creek, DIC was the major loss of carbon from the terrain to the surface water system. In contrast,DOC was higher than DIC in Swedish rivers and organic carbon comprised the majority of the carbon flux (Humborg *et al*., 2010). Large Siberian rivers are also richer in DIC than DOC. The Yukon River Basin experienced changes in flow paths due to the permafrost thawing and this alteration is believed to further decrease the DOC export and increase the DIC export (Walvoord and Striegl, 2007; Lyon and Destouni, 2010; Lyon *et al.*, 2010).

Conclusion

This research examined the impact of seasonal variations in runoff process on streamwater hydrochemistry in Wolf Creek Research Basin, Yukon, Canada. Various methods were applied to characterize this watershed, which is underlain by discontinuous permafrost. This thesis is different from others in the multiple methods utilized to characterize the runoff generation and hydrochemistry. Although there were previous studies using hydrometric, hydrochemical and isotopic data in similar catchments, this is the first one to combine tritium concentrations and radiocarbon concentrations as hydrochemical tracers.

Before the melt, the Wolf Creek streamwater contained relatively high concentrations of dissolved ions provided by baseflow sourced in groundwater. In late May, meltwater infiltrated into the soil, acquired soil DOC and discharged to the stream via near-surface soil pathways. Precipitation was a minor contributor to the runoff. The geochemical results were used to develop a three-component mixing model to describe seasonal variations in Wolf Creek streamwater. Streamwater in Wolf Creek is a mixture of groundwater, soilwater and precipitation. The soilwater and precipitation were much less concentrated in dissolved ions than the groundwater, and acted to dilute baseflow, while increasing total discharge during the spring freshet. Peak discharges occurred in June with the soilwater providing the largest contribution to the stream flow, exceeding the groundwater. However, towards the end of the freshet, soilwater contributions were declining while that of groundwater was still surging. The aqueous geochemistry and increased discharge of goundwater during the freshet is probably due to increased soilwater infiltration into the groundwater reservoir at this time

compared to that before the melt. Superimposed on this overall trend was a series of three soilwater peaks of uncertain origin. After June 24 both soilwater and groundwater discharge declined, with soilwater decline being more rapid. so that groundwater dominated the hydrograph again.

The geochemical data, in particular the K: Ca ratio, provided information to distinguish the baseflow (weathering zone) from the soilwater (organic zone). Stable isotope data were used for hydrograph separation to determine the contribution from each end-member. The tritium concentrations suggested a fast-moving hydrogeological system in Wolf Creek Research Basin. The application of carbon isotopes (^{13}C and ^{14}C) as tracers was an innovation for studying Wolf Creek Research Basin. The results showed the baseflow was enriched in both ^{14}C and ^{13}C as well as DIC. DIC was responsible for 70% to 90% of carbon export from the catchment.

In the summary, the combination of hydrometric, isotopic and hydrochemical data shed light on the exploration of the runoff process and the groundwater behavior in Wolf Creek Research Basin. Results from this study contribute to a better understanding of temporal variations in the streamwater flux and composition. Multiple methods facilitated development of a three-component mixing model for the runoff generation. It is important that isotopic and geochemical tracers can help validate and modify the conceptual model built on discharge data. The application for employing multiple analytic methods, like this study in Wolf Creek Research Basin, should be explored for different temporal and spatial scale.

Future Work

Although the study for this thesis was over, there are some more aspects should be further investigated to enhance the understanding of hydrology and hydrogeology in permafrost watersheds. Climate change in sub-arctic areas directly relates to the behavior of groundwater in watersheds like Wolf Creek Research Basin. How the global warming will affect the permafrost and groundwater in Wolf Creek can be explored by continuous sampling in the stream. It would be better if groundwater samples can be taken within the watershed. To achieve this work, groundwater wells need to be developed, or groundwater springs need to be found. However, the threshold for using groundwater samples to interpret stream flow is to make sure this is the groundwater recharge Wolf Creek. Groundwater samples were also taken during my study period, but their outlets were uncertain. Continuous and long-term sampling in the stream can quantify the variations in composition and contribution from groundwater.

More methods should be developed to advance the study for groundwater behavior. Noble gas methods would be a good choice in this case. Utting (2011) set a good example for this method conducted in University of Ottawa. The solubility of noble gases can indicated the recharge temperature of groundwater, ideally neon, argon, krypton and xenon (Kipfer et al., 2002; Utting, 2011). Old groundwater can also be dated by helium.

Another aspect in this study that could be improved in future is to work a wider sampling network in the watershed to improve mixing end-member characterization. There are large

temporal and spatial uncertainty existed in limited samples from the catchment. Hydrogeology transition from the source to the outlet can be discovered by adding samples along the flow path.

References

Anderson, L., Abbott, M. B., Finney, B. P., and Burns, S. J. (2005). Regional Atmospheric Circulation Change in the North Pacific During the Holocene Inferred from Lacustrine Carbonate Oxygen Isotopes, Yukon Territory, Canada. *Quaternary Research, 64(1),* 21-35.

Balcarczyk, K. L., Jones Jr, J. B., Jaffé, R., and Maie, N. (2009). Stream Dissolved Organic Matter Bioavailability and Composition in Watersheds Underlain with Discontinuous Permafrost. *Biogeochemistry, 94(3),* 255-270.

Berner, R. A. and Lasaga, A. C. (1989). Modeling the Geochemical Carbon Cycle. *Scientific American (USA), 260(3).*

Boucher, J. L. (2009). A Case Study Evaluating Runoff Generation in a Subarctic Catchment Using Stable Isotope, Hydrochemical and Hydrometric Data. Master Thesis. Carleton University, Ottawa, Ontario, Canada.

Boucher, J. L., and Carey, S. K. (2010). Exploring Runoff Processes Using Chemical, Isotopic and Hydrometric Data in a Discontinuous Permafrost Catchment. *Hydrology Research, 41.6,* 508 - 519.

Brown, R. D. and Braaten, R. O. (1998). Spatial and Temporal Variability of Canadian Monthly Snow Depth, 1946–1995. *Atmos. Ocean, 36,* 37– 54.

Buttle, J. M. and Sami, K. (1990). Recharge Processes during Snowmelt: an Isotopic and Hydrometric Investigation. *Hydrological Processes, 4(4),* 343-360.

Carey, S. K. and Quinton, W. L. (2005). Evaluating Runoff Generation During Summer

Using Hydrometric, Stable Isotope, and Hydrochemical Methods in A Discontinuous Permafrost Alpine Catchment. *Hydrology Process. 19,* 95–114.

Carey, S. K. and Woo, M. K. (2001). Spatial Variability of Hillslope Water Balance, Wolf Creek Basin, Subarctic Yukon. *Hydrology Process. 15*, 3113–3132.

Carey, S. K., Boucher, J. L., and Duarte, C. M. (2013). Inferring Groundwater Contributions and Pathways to Streamflow During Snowmelt Over Multiple Years in a Discontinuous Permafrost Subarctic Environment (Yukon, Canada). *Hydrogeology Journal, 21*, 67-77.

Carey, S. K., DeBeer, C. M. (2008). Rainfall-Runoff Hydrograph Characteristics in A Discontinuous Permafrost Watershed and Their Relation to Ground Thaw. In *Proc., Ninth Int. Conf. on Permafrost. Fairbanks, AL, 29,* 233-238.

Carey, S.K**.** (2003). Dissolved Organic Carbon Fluxes in a Discontinuous Permafrost Subarctic Alpine Catchment. *Permafrost and Periglacial Processes, 14.* 161-171.

Carey, S.K. and Quinton, W. (2004). Evaluating Snowmelt Runoff Generation in a Discontinuous Permafrost Catchment Using Stable Isotope, Hydrochemical and Hydrometric Data. *Nordic Hydrology, 35*, 309-324.

Clark, I. and Fritz, P. (1997). Environmental Isotopes in Hydrogeology. Lewis Publishing, New York.

Clever, H.L. (1979). "IUPAC Solubilities: Krypton, Xenon, Radon." Pergamon Press, Oxford.

Cooper, L. W., Solis, C., Kane, D. L. and Hinzman, L. D. (1993) Application of Oxygen-18

Tracer Techniques to Arctic Hydrological Processes. *Arct. Alp. Res. 25*, 247–255.

Coultish, T. L. and Lewkowicz, A. G. (2003). Palsa Dynamics in a Subarctic Mountainous Environment, Wolf Creek, Yukon Territory, Canada. In: *Permafrost, Proceedings of the Eighth International Conference on Permafrost*, 21–25 July 2003, Zurich, Switzerland, PhillipsM, SpringmanSM, ArensonLU (eds). A.A. Balkema: Lisse*;* 163–168.

Dewalle, D. R., Swistock, B. R., and Sharpe, W. E. (1988). Component Tracer Model for Stormflow on a Small Appalachian Forested Catchment. *J. Hydrol.*, 104, 301– 310.

Dewalle, D. R., Swistock, B. R., and Sharpe, W. E. (1988). Three-component Tracer Model for Stormflow on a Small Appalachian Forested Catchment. *Journal of Hydrology, 104(1)*, 301-310.

Dingman, S. L. (1971). *Hydrology of the Glenn Creek Watershed Tanana River Basin, Central Alaska* (No. CRREL-RR-297). Cold Regions Research and Engineering Lab Hanover NH.

Douglas, T. A., Blum, J. D., Guo, L., Keller, K., and Gleason, J. D. (2012). Hydrogeochemistry of Seasonal Flow Regimes in the Chena River, a Subarctic Watershed Draining Discontinuous Permafrost in Interior Alaska (USA). *Chemical Geology.* 335, 48-62.

Dyke, L. D. (2001). Contaminant Migration through the Permafrost Active Layer, Mackenzie Delta Area, Northwest Territories. *Canada. Polar Record, 37(202)*, 215-228.

Ednie, M. (2003). Evaluation of the Basal Temperature of Snow (BTS) Method to Map Permafrost in Complex Mountainous Terrain, Wolf Creek, Y.T. MSc Thesis, University of

Ottawa, Ontario, Canada

Elsenbeer, H., Lack, A., and Cassel, K. (1995). Chemical Fingerprints of Hydrological Compartments and Flow Paths at La Cuenca, Western Amazonia. *Water Resour. Res., 31(12),* 3051–3058.

Environment Canada. (2012). Historical Weather. Retrieved from: http://climate.weather.gc.ca/climateData/dailydata_e.html?StationID=1617

Francis, S. (1997). Data Integration and Ecological Stratification of Wolf Creek Watershed, South-Central Yukon. Report prepared for Indian & Northern Affairs Canada and Agriculture Canada. Applied Ecosystem Management Ltd., Whitehorse, 23.

Frey, K. E., Siegel, D. I., and Smith, L. C. (2007). Geochemistry of West Siberian Streams and Their Potential Response to Permafrost Degradation. *Water Resources Research, 43*(3).

Genereux, D.P. (1998) .Quantifying Uncertainty in Tracer-Based Hydrograph Separations. *Water Resources Research. 34*, 915–919.

Geyh, M. A. (*2000*). An Overview of ^{14}C Analysis in the Study of Groundwater. *Radiocarbon, 42,* 99–114.

Gibson, J. J., Edwards, T. W. D., Birks, S. J., St Amour, N. A., Buhay, W. M., McEachern, P., Wolfe, B. B. and Peters, D. L. (2005). Progress in Isotope Tracer Hydrology in Canada. *Hydrol. Process., 19,* 303–327.

Gröning, M., Taylor, C. B., Winckler, G., Auer, R. and Tatzber, H. (2001). Sixth IAEA Intercomparison of Low-Level Tritium Measurements in Water (TRIC2000). Report IAEA, Vienna.

Heginbottom, J. A., Dubreuil, M. A., and Harker, P. T. (1995). Canada- Permafrost (1:7 500 000 scale). In the National Atlas of Canada, 5th edn. Ottawa: National Resources Canada, sheet MCR 4177.

Hill, R. P. (1982). Report on Whitehorse Coal. Whitehorse Coal Corporation, Whitehorse, Yukon.

Hinton, M. J. S., Schiff, S. L., and English, M. C. (1994). Examining the Contributions of Glacial Till Water to Storm Runoff Using Two-component and Three-component Hydrograph Separations. *Water Resour. Res., 30*, 983– 993.

Hinzman, L. D., Kane, D. L., Yoshikawa, K., Carr, A., Bolton, W. R., and Fraver, M. (2003). Hydrological Variations among Watersheds with Varying Degrees of Permafrost. In *Proceedings of the Eighth International Conference on Permafrost*, 21-25.

Hinzman, L.D., Goering, D.J., and Kane, D.L. (1998). A Distributed Thermal Model for Calculating Temperature Profiles and Depth of Thaw in Permafrost Regions. *Journal of Geophysical Research 103 (D22), 28*,975–28,991.

Hinzman, L.D., Kane, D.L., Gieck, R.E., and Everett, K.R. (1991). Hydrologic and Thermal Properties of the Active Layer in the Alaskan Arctic. *Cold Regions Science and Technology 19 (2)*, 95–110.

Hoeg, S., Uhlenbrook, S., and Leibundgut, C. (2000). Hydrograph Separation in a Mountainous Catchment—Combining Hydrochemical and Isotopic Tracers. *Hydrological Processes, 14(7),* 1199-1216.

Humborg, C., Mörth, C., Sundbom, M., Borg, H., Blenckner, T., Giesler, R., and Ittekkot, V. (2010). CO_2 Supersaturation along the Aquatic Conduit in Swedish Watersheds as Constrained by Terrestrial Respiration, Aquatic Respiration and Weathering. *Global Change Biology, 16(7),* 1966-1978.

Janowicz, J. R. (1990). Regionalization of Low Flows in Yukon Territory. In *Northern Hydrology: Selected Perspectives,* Prowse TD, Omman-ney CSL (eds). Proceedings of the Northern Hydrology Symposium, 10 – 12 July, 1990, National Hydrology Research Institute: Saskatoon; 141 – 150.

Janowicz, J. R. (1986). A Methodology for Estimating Design Peak Flows for Yukon Territory. In *Proceedings of Cold Regions Hydrology Symposium* (edited by D.L. Kane). American Water Resources Association, 313-320.

Jasek, M. and Ford, G. (1997). Coal Lake Outlet Freeze-Up, Containment of Winter Inflows and Estimates of Related Outburst Flood on Wolf Creek, Yukon Territory. 65th Annual Western Snow Conference.

Jorgenson, M. T., Shur, Y. L. and Pullman, E. R. (2006). Abrupt Increase in Permafrost Degradation in Arctic Alaska. *Geophysical Research Letters, 33(2),* L02503.

Kane, D. L. and Stein, J. (1983). Water movement into seasonally frozen soils. *Water Resources Research, 19*(6), 1547-1557.

Kane, D. L., Hinzman, L. D. and Zarling, J. P. (1991). Thermal Response of the Active Layer to Climatic Warming in a Permafrost Environment. *Cold Regions Science and Technology 19 (2)*, 111–122.

Kane, D. L., McNamara, J. P., Yang, D., Olsson, P. Q. and Gieck, R. E. (2003). An Extreme Rainfall/Runoff Event in Arctic Alaska. *Journal Hydrometeorol 5*, 1220–1228.

Kaser, G., J. G. Cogley, M. B. Dyurgerov, M. F. Meier, and A. Ohmura (2006), Mass Balance of Glaciers and Ice Caps: Consensus Estimates for 1961 – 2004. *Geophysical Research Letters, 33*, L19501.

Kipfer, R., Aeschbach-Hertig, W., Peeters, F., and Stute, M. (2002). Noble gases in Lakes and Ground Waters. *Reviews in mineralogy and geochemistry*, *47*(1), 615-700.

Kokelj, S. V., and Burn, C. R. (2005). Near-Surface Ground Ice in Sediments of the Mackenzie Delta, Northwest Territories, Canada. *Permafrost and Periglacial Processes*, *16*(3), 291-303.

Kokelj, S. V., Smith, C. A. S. and Burn, C. R. (2002). Physical and Chemical Characteristics of the Active Layer and Permafrost, Herschel Island, Western Arctic Coast, Canada. *Permafrost and Periglacial Processes, 13*, 171–185.

Kokelj, S.V. and Lewkowicz, A.G. (1999). Salinization of Permafrost Terrain Due To Natural Geomorphic Disturbance, Fosheim Peninsula, Ellesmere Island. *Arctic, 52*, 372–385.

Kokelj, S.V., and Burn, C.R. (2003). Ground Ice and Soluble Cations in Near-Surface Permafrost, Inuvik, Northwest Territories. *Permafrost and Periglacial Processes, 14*, 275–

289.

Lacelle, D. (2011). On the $\delta^{18}O$, δD and D-excess relations in meteoric precipitation and during equilibrium freezing: theoretical approach and field examples. *Permafrost and Periglacial Processes*, 22, 13-25.

Lachenbruch, A. H. and Marshall, B. V. (1986). Changing Climate: Geothermal Evidence from Permafrost in the Alaskan Arctic. *Science*, *234*(4777), 689-696.

Langmuir, D. (1997). Aqueous Environmental Geochemistry. Pretice-Hall Inc.. New Jersey.

Laudon, H., and Slaymaker, O. (1997). Hydrograph Separation Using Stable Isotopes, Silica and Electrical Conductivity: An Alpine Example. *Journal of Hydrology*, *201*(1), 82-101.

Laudon, H., Seibert, J., Köhler, S. and Bishop, K. (2004). Hydrological Flow Paths During Snowmelt: Congruence Between Hydrometric Measurements and Oxygen 18 in Meltwater, Soil Water, and Runoff. *Water Resour. Res., 40(3).*

Leibman, M. O. and Streletskaya, I. D. (1997). Landslide Induced Changes in the Chemical Composition of Active-Layer Soils and Surface-Water Runoff, Yamal Peninsula, Russia. In *Proceedings of the International Symposium on Physics, Chemistry and Ecology of Seasonally Frozen Soils, Fairbanks, Alaska,* 10–12 June 1997. Edited by I.K. Iskandar, E.A. Wright, J.K. Radke, B.S. Sharratt, P.H. Groenevelt, and L.D. Hinzman. CRREL Special Report 97-10, Cold Regions Research and Engineering Laboratory (CRREL), Hanover, N.H., 120–126.

Lewkowicz, A. G. and Ednie, M. (2004). Probability Mapping of Mountain Permafrost Using the BTS Method, Wolf Creek, Yukon Territory, Canada. *Permafrost Periglac. Process.*

15, 67–80.

Lyon, S. W., and Destouni, G. (2010). Changes in Catchment-scale Recession Flow Properties in Response to Permafrost Thawing in the Yukon River Basin. *International Journal of Climatology*, *30(14)*, 2138-2145.

Lyon, S. W., Mörth, M., Humborg, C., Giesler, R., and Destouni, G. (2010). The Relationship between Subsurface Hydrology and Dissolved Carbon Fluxes for a Sub-Arctic Catchment. *Hydrology and Earth System Sciences*, *14(6)*, 941-950.

MacLean, R.., Oswood, M. W., Irons, J. G., III and McDowell, W. H. (1999). the Effect of Permafrost On Stream Biogeochemistry: A Case Study of Two Streams in the Alaskan (U.S.A.) Taiga. B*iogeochemistry 47*, 239–267.

McCartney, S. E., Carey, S. K., and Pomeroy, J. W. (2006). Intra‐basin Variability of Snowmelt Water Balance Calculations in a Subarctic Catchment. *Hydrological Processes*, *20(4)*, 1001-1016.

McGlynn, B. L., McDonnell, J. J., Shanley, J. B., and Kendall, C. (1999). Riparian Zone Flowpath Dynamics During Snowmelt in a Small Headwater Catchment. *J. Hydrol.*, *222*, 75– 92.

McIntosh, J. C., Schlegel, M. E. and Person, M. (2012). Glacial Impacts on Hydrologic Processes in Sedimentary Basins: Evidence from Natural Tracer Studies. *Geofluids*, *12*, 7–21.

McNamara, J. P., Kane, D. L., and Hinzman, L. D. (1997). Hydrograph Separations in an

Arctic Watershed Using Mixing Model and Graphical Techniques. *Water Resources Research, 33(7),* 1707-1719.

Metcalfe, R. A., and Buttle, J. M. (1999). Semi-distributed Water Balance Dynamics in a Small Boreal Forest Basin. *Journal of Hydrology, 226(1),* 66-87.

Michel, F.A. and Fritz, P. (1978). Environmental Isotopes in Permafrost Related Waters along the Mackenzie Valley Corridor. *Proc. 3rd Int. Conf. on Permafrost,* Natl. Res. Council Can., 1, 207-21 1.

Monteith, S. S., Buttle, J. M., Hazlett, P. W., Beall, F. D., Semkin, R. G. and Jeffries, D. S. (2006). Paired-basin Comparison of Hydrologic Response in Harvested and Undisturbed Hardwood Forests during Snowmelt in Central Ontario: II. Streamflow Sources and Groundwater Residence Times. *Hydrol. Process, 20*. 1117–1136.

Muskett, R. R., and Romanovsky, V. E. (2009). Groundwater Storage Changes in Arctic Permafrost Watersheds from GRACE and *in-situ* Measurements. *Environmental Research Letters, 4(4),* 045009.

Neuman, C. M. (1989). Kinetic Energy Transfer through Impact and Its Role in Entrainment by Wind of Particles from Frozen Surfaces. *Sedimentology, 36(6),* 1007-1015.

NRC (National Research Council of Canada). (1988). Glossary of Permafrost and Related Ground Ice Terms, Associate Committee on Geotechnical Research. *Permafrost Subcommittee, 156.* Government of Canada.

Obradovic, M. M. and Sklash, M. G. (1986). An Isotopic and Geochemical Study of Snowmelt Runoff in a Small Arctic Watershed. *Hydrology Process, 1,* 15–30.

Ogunkoya, O. O., and Jenkins, A. (1993). Analysis of Storm Hydrograph and Flow Pathways Using a 3-component Hydrograph Separation Model. *J. Hydrol., 142*, 71– 88.

Petrone, K. C., Jones, J. B., Hinzman, L. D., and Boone, R. D. (2006). Seasonal Export of Carbon, Nitrogen, and Major Solutes from Alaskan Catchments with Discontinuous Permafrost. *Journal of Geophysical Research: Biogeosciences (2005–2012), 111*(*G2)*, G02020.

Péwé, T.L., and Sellmann, P.V. (1973). Geochemistry of Permafrost and Quaternary Stratigraphy. *in Permafrost:* the North American contribution to the 2nd International Conference, Yakutsk, U.S.S.R. National Academy of Science Press, Washington, D.C., 166–170.

Pinder, G. F. and Jones, J. F. (1969). Determination of the Ground-water Component of Peak Discharge from the Chemistry of Total Runoff. *Water Resources Research, 5(2),* 438-445.

Pomeroy, J. (2004). CEOP Hydrology Reference Sites: Wolf Creek, Yukon Territory, Canada. Retrieved from: http://hydrology.princeton.edu/~luo/ceop/wolf_creek.php

Quinton, W. L. and Gray, D. M. (2001). Estimating Subsurface Drainage From Organic-Covered Hillslopes Underlain By Permafrost: Toward A Combined Heat and Mass Flux Model. *IAHS Publication*, 333-342.

Quinton, W. L., Shirazi, T., Carey, S. K. and Pomeroy, J. W. (2005), Soil Water Storage and Active-Layer Development in a Sub-Alpine Tundra Hillslope, Southern Yukon Territory, Canada. *Permafrost Periglac. Process, 16,* 369–382.

References

Rice, K. C., *and* Hornberger, G. M. (1998). Comparison of Hydrochemical Tracers to Estimate Source Contributions to Peak Flow in a Small, Forested, Headwater Catchment. *Water Resour. Res.*, *34*(*7*), 1755–1766.

Riordan, B., Verbyla, D., and McGuire, A. D. (2006). Shrinking Ponds in Subarctic Alaska Based on 1950–2002 Remotely Sensed Images. *Journal of Geophysical Research: Biogeosciences (2005–2012), 111(G4).*

Rouse, W.R. (2000). Progress in Hydrological Research in the Mackenzie GEWEX Study. *Hydrological Processes 14,* 1667–1685.

Seguin, M. (1998) Regolith Profiles and Permafrost Distribution of the Wolf Creek Watershed, Yukon Territory, Canada. in *Institute National de la Recherche Scientifique*, INRS-EAU, Québec, Canada

Seguin, M. K., Stein, J., Nilo, O., Jalbert, C. and Ding, Y. (1999). Hydrogeophysical Investigation of the Wolf Creek Watershed, Yukon Territory, Canada. In *Wolf Creek Research Basin: Hydrology, Ecology, Environment.* Pomeroy JW, Granger RJ (eds). National Water Re-search Institute, Saskatoon, 33–43.

Serreze, M. C., Walsh, J. E., Chapin III, F. S., Osterkamp T., Dyurgerov, M., Romanovsky, V., Oechel, W. C., Morison, J., Zhang, T., and Barry, R. G. (2000), Observational Evidence of Recent Change in the Northern High-Latitude Environment. *Climate Change, 46,* 159–207.

Shanley, J. J., Kendall, C., Smith, T. E., Wolock, D. M. and McDinnell, J. J. (2002). Controls

on Old and New Water Contributions To Stream Flow At Some Nested Catchments in Vermont, USA. *Hydrology Process 16*,589–609.

Slaughter, C. W. and Kane, D. L. (1979). Hydrologic Role of Shallow Organic Soils in Cold Climates. In *Canadian Hydrology Symposium:* 79 Cold Climate Hydrology. National Research Council of Canada, Vancouver, 380-389.

Slaughter, C. W., Hilgert, J. W. and Culp, E. H. (1983). Summer Streamflow and Sediment Yield from Discontinuous-Permafrost Headwaters Catchments. In: *Proc. Fourth International Conference on Permafrost*. National Academy Press, Washington, DC, 1172–1177.

Spence, C., Kokelj, S. V., Ehsanzadeh, E. (2011). Precipitation Trends Contribute To Streamflow Regime Shifts in Northern Canada. In: *Cold region hydrology in a changing climate.* IAHS Publ. 346, IAHS, Wallingford, UK, 3–8.

St-Jean, G. (2003). Automated Quantitative and Isotopic (^{13}C) Analysis of Dissolved Inorganic Carbon and Organic Carbon in Continuous-flow Using a Total Organic Carbon Analyser. *Rapid Communication in Mass Spectrometry, 17,* 418-428.

Striegl, R. G., Aiken, G. R., Dornblaser, M. M., Raymond, P. A., and Wickland, K. P. (2005). A Decrease in Discharge-Normalized DOC Export by the Yukon River During Summer Through Autumn. *Geophysical Research Letters, 32(21),* L21413.

Tolstikhin, N. I., Tolstikhin, O. N. (1976). Groundwater and Surface Water in the Permafrost Region (Translation). *Inland Waters Directorate Tech Bull 97*, Ottawa, Ontario, 22

Utting, N. (2012). *Geochemistry and Noble Gases of Permafrost Groundwater and Ground Ice in Yukon and the Northwest Territories, Canada*. PhD Thesis, University of Ottawa, Ottawa, Ontario, Canada..

Utting, N., Clark, I., Lauriol, B., Wieser, M. and Aeschbach-Hertig, W. (2012). Origin and Flow Dynamics of Perennial Groundwater in Continuous Permafrost Terrain using Isotopes and Noble Gases: Case Study of the Fishing Branch River, Northern Yukon, Canada. *Permafrost Periglac. Proces., 23*, 91–106.

van Everdingen, R. O. (1990). Chapter 4: Ground-water Hydrology. in: *Prowse TD*, Ommanney CSL (eds) Northern hydrology; Canadian perspectives. National Hydrology Research Institute, Environment Canada, NHRI Science Report No. 1, 77–101

Walvoord, M. A., and Striegl, R. G. (2007). Increased Groundwater to Stream Discharge From Permafrost Thawing in the Yukon River Basin: Potential Impacts on Lateral Export of Carbon and Nitrogen. *Geophysical Research Letters, 34(12),* L12402.

Weiss, R. (1970). The Solubility of Nitrogen, Oxygen and Argon in Water and Seawater. *Deep-sea Research 17,* 721-735.

Weiss, R. (1971). Solubility of Helium and Neon in Water and Seawater. *Journal of Chemical and Engineering Data 16,* 235–241.

Weiss, R. (1978). Solubility of Krypton in Water and Sea Water. *Journal of chemical and engineering data, 23*, 69-72.

Williams, J. R. and Waller, R. M. (1966). Groundwater Occurrence in Permafrost Regions of Alaska. In: *Proceedings of the 1st international conference on permafrost*, Lafayette.

National Academy of Sciences, Washington, DC, 159–164.

Woo, M. K. (1986) Permafrost Hydrology in North America. *Atmos. Ocean 24*, 201-234.

Woo, M. K. (2000). Permafrost and Hydrology. In: *the Arctic: Environment, People, Policy*. Nuttall, M. and Callaghan, T.V. (eds). Harwood, Newark, NJ, 57–96.

Woo, M. K**.** (2012). *Permafrost Hydrology.* Springer, Heidelberg, 563.

Woo, M. K. and Winter, T. C. (1993). The Role of Permafrost and Seasonal Frost in the Hydrology of Northern Wetlands in North America. *Journal of Hydrology 141*, 5-31.

Yang, Z. P., Ou, Y. H., Xu, X. L., Zhao, L., Song, M. H., & Zhou, C. P. (2010). Effects of Permafrost Degradation on Ecosystems. *Acta Ecologica Sinica, 30(1),* 33-39.

Zhu C, Murphy W. M. (2000). On Radiocarbon Dating of Ground Water. *Ground Water, 38,* 802–4.

Appendix: Geochemistry and Isotope Analysis Results

Appendix: Geochemistry and Isotope Analysis Results

SampleID	pH	Al (ppm)	Na (ppm)	K (ppm)	Mg (ppm)	Ca (ppm)	Fe (ppm)	Ba (ppm)	Cl (ppm)	SO4 (ppm)	NO2 (ppm)	S (ppm)	Si (ppm)	DIC (ppm C)	13C DIC (‰,VPDB)	DOC (ppm C)	13C DOC (‰,VPDB)	Delta 18O (‰,VSMOW)	Delta 2H (‰,VSMOW)	Tritium (TU)	pMC (%)	Delta 14C (‰)
Snow	5.95	0.00	0.05	0.04	0.02	0.16	0.00	0.00	0.07	0.04	0.05	0.01	0.03	0.38	-17.98	0.75	-35.34	-20.87	-163.22			
WCRB Spring	7.07	0.01	2.68	0.33	3.24	7.92	0.03	0.01	0.08	1.71	1.96	0.70	9.56	9.10	-18.58	1.61	-35.68	-22.30	-170.62			
WCRB5	7.03	0.03	1.90	0.11	1.47	6.51	0.17	0.02	0.09	1.86	1.28	0.79	4.11	6.63	-14.74	6.53	-27.26	-21.51	-166.17			
Golden Horn Lake	7.34	0.03	1.83	3.09	1.93	6.57	0.03	0.03	2.64	1.53	1.39	0.70	3.44	5.83	-10.90	7.43	-27.19	-20.63	-166.46			
Coal Lake Drainage	6.99	0.10	1.47	0.11	0.41	2.04	0.05	0.02	0.09	0.44	0.59	0.20	3.95	2.69	-11.79	4.79	-27.14	-22.11	-172.51			
POND1	7.64	0.03	1.85	0.41	1.56	5.01	0.01	0.02	0.06	2.51	1.19	`	3.50	4.22	-11.69	3.69	-24.75	-19.57	-161.76			
WCRB1	7.46	0.01	1.81	0.18	1.67	5.71	0.05	0.01	0.05	4.35	1.21	1.68	4.59	4.06	-9.01	1.10	-25.84	-22.03	-171.34			
WCRB10	7.36	0.02	1.98	0.12	1.08	4.26	0.01	0.01	0.02	3.99	0.96	1.50	5.67	3.28	-10.71	1.03	-26.60	-22.28	-172.76			
POND2	7.09	0.02	3.30	0.32	3.47	10.38	0.71	0.02	0.10	4.89	1.98	1.89	5.20	9.74	-11.90	6.44	-25.91	-21.89	-173.27			
WCRB3	7.44	0.01	1.73	0.30	1.78	6.87	0.01	0.02	0.06	5.40	1.32	2.03	4.55	5.00	-11.76	2.03	-33.30	-22.28	-170.05			
Crk1	7.69	0.01	2.02	0.18	1.95	6.59	0.41	0.02	0.06	4.25	1.41	1.60	4.91	5.46	-9.39	1.07	-24.57	-22.26	-169.73			
Crk2	7.14	0.01	2.43	0.30	2.03	6.38	0.24	0.01	0.06	3.48	1.43	1.40	5.56	5.91	-13.07	3.00	-27.04	-22.13	-171.89			
POND5	8.67	0.03	5.16	1.08	7.81	33.92	0.06	0.06	0.52	20.90	3.96	7.96	5.62	29.57	-7.37	2.36	-32.36	-19.29	-159.35			
Lake1	8.39	0.03	16.48	3.70	32.44	38.44	0.03	0.04	1.98	120.60	4.34	45.96	3.42	35.45	-3.40	16.69	-25.88	-14.55	-139.13			
POND3	8.46	0.02	11.12	1.99	31.06	66.50	0.02	0.03	0.76	170.53	4.23	64.60	3.43	35.92	-5.46	14.78	-26.05	-17.46	-155.14			
POND4	8.48	0.05	11.48	3.14	40.47	70.77	0.05	0.07	1.18	244.78	3.70	92.13	1.29	29.61	-2.35	2.35	-36.13	-11.72	-124.63			

SampleID	pH	Al (ppm)	Na (ppm)	K (ppm)	Mg (ppm)	Ca (ppm)	Fe (ppm)	Ba (ppm)	Cl (ppm)	SO4 (ppm)	NO2 (ppm)	S (ppm)	Si (ppm)	DIC (ppm C)	13C DIC (‰,VPDB)	DOC (ppm C)	13C DOC (‰,VPDB)	Delta 18O (‰,VSMOW)	Delta 2H (‰,VSMOW)	Tritium (TU)	pMC (%)	Delta 14C (‰)
WC Camp Spring	7.33	0.03	8.20	1.81	16.28	64.53	0.01	0.09	2.59	62.29	5.30	23.31	5.75	51.47	-10.90	1.41	-33.14	-19.63	-161.61			
WC Camp Well	8.08	0.03	5.83	1.67	14.00	50.68	0.09	0.07	0.72	40.77	4.91	15.57	4.73	39.18	-10.64	1.15	-34.89	-20.81	-166.56			
Coal Lake	8.29	0.00	2.56	0.57	5.60	24.86	0.00	0.13	0.11	10.81	3.23	4.11	3.14	17.51	-8.13	2.82	-24.20	-21.70	-168.81			
WC Outflow	8.22	0.00	2.58	0.54	5.51	25.20	0.01	0.13	0.11	10.83	3.26	4.16	3.17	16.49	-7.76	2.86	-25.79	-21.42	-169.50			
WCRB9	8.00	0.01	2.69	0.61	5.90	25.69	0.02	0.12	0.12	11.19	3.32	4.27	3.38	19.01	-8.64	2.96	-26.17	-21.46	-169.83			
WCRB6	8.10	0.01	2.95	2.36	5.72	22.69	0.01	0.08	0.58	10.02	3.12	3.80	4.56	16.08	-7.93	4.83	-26.34	-21.82	-169.42			
WCRB6-2	8.30	0.03	3.62	0.72	5.81	23.44	0.03	0.10	0.14	10.58	3.25	4.03	5.15	17.12	-8.16	2.55	-26.23	-21.87	-169.47			
WC @ Alaska Hwy	7.77	0.00	2.97	0.68	5.85	23.16	0.01	0.07	0.12	10.28	3.19	3.91	4.59	16.65	-7.91	3.04	-30.99	-21.77	-171.19			
WCRB14	8.20	0.03	3.67	1.07	5.85	24.04	0.10	0.09	0.51	10.91	5.29	4.19	5.17	17.88	-8.50	3.69	-32.87	-21.87	-168.66			
WC April 28	7.84	0.01	3.56	0.91	7.24	27.99	0.01	0.07	0.24	13.82	3.64	5.32	4.79	21.31	-9.47	3.99	-26.44	-22.25	-166.66	8.64	90.61	-86.90
WC May 7	7.88	0.01	3.61	0.93	7.31	28.43	0.03	0.07	0.56	13.52	3.73	5.12	4.89	21.87	-8.15	2.02	-26.02	-22.27	-167.92	7.89	89.56	-97.50
WC May 17	7.90	0.01	3.50	0.98	7.23	28.46	0.07	0.08	0.23	12.20	3.72	4.66	4.90	21.72	-8.72	2.81	-26.89	-22.58	-168.57	7.98		
WC May 27	7.69	0.02	2.07	0.96	3.96	15.47	0.10	0.05	0.21	5.50	2.44	2.17	3.65	12.31	-11.21	5.48	-27.79	-23.07	-170.25	6.48	92.73	-65.60

SampleID	pH	Al (ppm)	Na (ppm)	K (ppm)	Mg (ppm)	Ca (ppm)	Fe (ppm)	Ba (ppm)	Cl (ppm)	SO4 (ppm)	NO2 (ppm)	S (ppm)	Si (ppm)	DIC (ppm C)	13C DIC (‰,VPDB)	DOC (ppm C)	13C DOC (‰,VPDB)	Delta 18O (‰,VSMOW)	Delta 2H (‰,VSMOW)	Tritium (TU)	pMC (%)	Delta 14C (‰)
WC June 2	7.50	0.02	2.19	0.77	3.96	15.05	0.07	0.04	0.17	5.98	2.41	2.31	4.12	12.92	-12.80	4.36	-26.07	-22.86	-168.98	9.87	71.91	-275.40
WC June 10	7.63	0.03	1.81	0.75	3.32	13.21	0.07	0.04	0.21	5.85	2.16	2.25	3.35	11.69	-12.20	8.99	-27.90	-22.62	-166.96	6.87	55.78	-437.90
WC June 18	7.30	0.01	2.54	0.77	4.58	18.49	0.02	0.06	0.27	7.85	2.78	3.02	4.29	16.23	-12.50	3.53	-25.48	-22.84	-169.08	9.11	65.92	-335.80
WC June 24	7.39	0.02	2.33	0.62	4.45	18.47	0.03	0.07	0.11	7.73	2.75	3.00	4.09	15.21	-12.22	2.99	-25.31	-22.72	-168.91	6.24	72.18	-272.60
WC July 1	7.42	0.01	2.64	0.71	5.10	20.75	0.01	0.07	0.15	8.96	2.97	3.48	4.50	16.84	-10.93	4.33	-27.57	-22.42	-168.47	7.82	72.63	-268.10
WC July 10	7.49	0.01	2.70	0.62	5.13	20.85	0.01	0.07	0.12	9.30	3.00	3.58	4.53	16.52	-10.61	2.42	-24.26	-22.14	-167.84	7.99	79.70	-196.90
WC July 19	7.81	0.01	2.72	0.66	5.01	20.86	0.40	0.07	0.13	9.31	3.00	3.63	4.45	16.54	-11.72	4.63	-25.10	-22.05	-168.08	7.06	81.21	-181.60
WC July 23	7.76	0.01	2.90	0.70	5.47	22.36	0.06	0.07	0.14	9.97	3.14	3.79	4.46	17.30	-9.56	4.16	-24.97	-21.98	-167.73	7.37	76.11	-233.10
WC Aug 2	7.65	0.01	2.99	0.67	5.56	23.23	0.02	0.07	0.13	10.51	3.24	3.99	4.52	17.89	-8.70	3.54	-25.63	-21.94	-167.54	4.63	74.69	-247.30
WC Aug 10	7.52	0.02	2.59	0.50	4.53	17.68	0.00	0.05	0.20	10.21	3.54	2.91	3.66	17.30	-8.35	3.13	-24.68	-21.72	-166.88	7.53	82.70	-166.70
WC Aug 14	7.62	0.01	2.59	0.49	4.65	18.57	0.00	0.05	0.19	10.84	3.64	3.03	3.68	18.49	-9.92	3.70	-25.94	-21.30	-166.90	7.87	79.91	-194.80

SampleID	pH	Al (ppm)	Na (ppm)	K (ppm)	Mg (ppm)	Ca (ppm)	Fe (ppm)	Ba (ppm)	Cl (ppm)	SO4 (ppm)	NO2 (ppm)	S (ppm)	Si (ppm)	DIC (ppm C)	13C DIC (‰,VPDB)	DOC (ppm C)	13C DOC (‰,VPDB)	Delta 18O (‰,VSMOW)	Delta 2H (‰,VSMOW)	Tritium (TU)	pMC (%)	Delta 14C (‰)
WC Aug 30	7.51	0.02	2.89	0.52	5.20	20.66	0.00	0.06	0.21	11.37	3.63	3.42	4.00	19.46	-8.87	7.78	-28.24	-21.36	-167.56	8.48	77.04	-223.70
WC Sep 12	7.66	0.00	3.02	0.47	5.18	20.47	0.00	0.06	0.19	11.19	3.73	3.50	3.75	18.73	-6.70	3.69	-25.98	-21.55	-168.00	8.33	84.34	-150.20
WC Oct 10	7.65	0.00	3.17	0.47	5.44	21.25	0.04	0.06	0.20	11.74	3.79	3.71	3.90	18.64	-8.05	5.23	-26.12	-21.49	-167.50	7.35	86.76	-125.70
P-June 3-10		0.00	0.16	0.15	0.06	0.44	0.01	0.00	0.17	0.22	0.15	0.13	0.03					-18.85	-154.68			
P-June 10-18		0.00	0.24	1.75	0.12	0.56	0.01	0.00	0.35	0.59	0.55	0.29	0.01	1.24	-18.14			-26.26	-211.49			
P-June 18-24		0.00	0.06	0.26	0.04	0.40	0.01	0.00	0.08	0.21	0.11	0.11	0.01	0.86	-22.4			-20.12	-164.87			
P-June 24-July 5		0.00	0.05	0.34	0.07	0.42	0.02	0.00	0.09	0.17	0.17	0.07	0.01	0.85	-23.34			-21.15	-170.10			
P-July 5-15		0.00	0.04	0.11	0.06	0.42	0.03	0.00	0.05	0.38	0.06	0.18	0.03	0.85	-25.55			-16.77	-130.63			
P-July 15-29		0.01	0.08	0.87	0.10	0.56	0.01	0.00	0.06	0.18	0.15	0.11	0.02	0.85	-23.34			-19.68	-162.12			
P-12-Aug		0.01	0.04	0.13	0.04	0.26	0.00	0.00	0.18	0.22	0.07	0.00	0.04	0.43	-17.54			-17.11	-133.76			
P-19-Aug		0.02	0.08	0.26	0.07	0.39	0.00	0.00	0.25	0.16	0.12	-0.01	0.06	2.26	-24.48			-15.53	-127.67			

SampleID	pH	Al (ppm)	Na (ppm)	K (ppm)	Mg (ppm)	Ca (ppm)	Fe (ppm)	Ba (ppm)	Cl (ppm)	SO4 (ppm)	NO2 (ppm)	S (ppm)	Si (ppm)	DIC (ppm C)	13C DIC (‰,VPDB)	DOC (ppm C)	13C DOC (‰,VPDB)	Delta 18O (‰,VSMOW)	Delta 2H (‰,VSMOW)	Tritium (TU)	pMC (%)	Delta 14C (‰)
P-24-Aug		0.01	0.02	0.08	0.01	0.13	0.00	0.00	0.15	0.22	0.00	-0.03	0.04	0.62	-22.26			-16.63	-132.68			
P-30-Aug		0.02	0.02	0.07	0.01	0.08	0.00	0.00	0.13	0.19	-0.01	-0.05	0.04	0.49	-23.79			-15.06	-116.16			